Available online at www.sciencedirect.com
SCIENCE DIRECT
Journal of Asian Earth Sciences 24 (2005) 495–515
Journal of Asian Earth Sciences
www.elsevier.com/locate/jaes

Cenozoic deformation in western Yunnan (China–Myanmar border)☆

Anne Socquet[a,b,*], Manuel Pubellier[a]

[a]Laboratoire de Géologie, CNRS UMR 8538, Ecole Normale Supérieure, 24 rue Lhomond, 75005 Paris, France
[b]Department of Earth Observation and Space Systems, Delft University of Technology, Kluyverweg 1, HS Delft 2629, The Netherlands

Accepted 29 March 2004

Abstract

In the present paper, we describe ductile and brittle deformation styles in western Yunnan and NE Myanmar, using field data and Landsat 7 imagery. We show that this complex area located at the northern termination of Sunda Plate (Three Rivers area) was wedged during the Tertiary between the left-lateral Ailao Shan/Chong Shan metamorphic belts to the east and the right-lateral Shan scarp/Gaoligong metamorphic belt in west. This triangular region therefore underwent the effects of these continental size ductile strike-slip faults separating major blocks with a dominant EW to ENE compression. Since the Late Miocene, date of the reversal of motion along the RRF, the incipient eastward motion of the Sunda block and the persisting right-lateral motion along its western boundary (Sagaing fault) created N–S compression and E–W to WNW extension underlined by left-lateral transtension along the Wanding/Nanting fault zones. At the same time, the Diangcan Shan, situated along strike the Ailao Shan metamorphic belt, was slightly impinged by the blocks extruded from the syntaxis and exhumed again from the Early Pliocene in accordance with this late and still active state of stress.

Keywords: Miocene; Pliocene; Tibetan plateau; Structural geology; Shear zones; GIS

1. Introduction

The Eastern Himalayan Syntaxis is a zone of escape characterized by a clockwise flow of material around the north-eastern edge of India (Holt et al., 1991). This flow of crustal material is accommodated of surface by large curved strike slip faults which delineate smaller crustal blocks (Ratschbacher et al., 1996; Wang et al., 1998) (Figs. 1 and 2). This escape tectonics ensures the transition from a compressional regime in the Himalayas to a right-lateral shear in Myanmar.

Such processes have been invoked in the eastern Alps which have been extruded eastward toward the western Pannonian basin (Ratschbacher et al., 1991) or in eastern Aegea (Jolivet, 2001) where westward escape of Anatolia is guided by the active north Anatolian fault at a rate of 2.5 cm/yr. Another local example of such rotational tectonics is the western Irian Jaya (Indonesia) where the Bird's Head block escapes westward with a rate of 7 cm/yr from the collision between Australia and the remnants of volcanics carried by the pacific plate (Pubellier and Ego, 2002).

In western Yunnan, the tectonic features are influenced by both the clockwise flow around the Eastern Himalayan Syntaxis, and the northern extension along splays of the Sagaing fault. Deformation is then distributed between strike-slip and normal faulting and a cylindric approach of the structures is not relevant. Lateral heterogeneities, partitioning of the deformation and the rotational tectonic styles have to be considered.

2. Geodynamic framework

2.1. Age of India Eurasia collision

Western Yunnan (China) is situated in the southern part of the Eastern Himalayan Syntaxis close to the Myanmar border (Figs. 1 and 2). This syntaxis can be considered as junction between India, Eurasia, Sunda and South China

☆ Originally submitted for 17 Himalaya-Tibet workshop.

* Corresponding author. Tel.: +31-152-78-2043; fax: +31-152-78-5322.
E-mail address: anne@deos.tudelft.nl (A. Socquet).

1367-9120/$ - see front matter © 2004 Elsevier Ltd. All rights reserved.
doi:10.1016/j.jseaes.2004.03.006

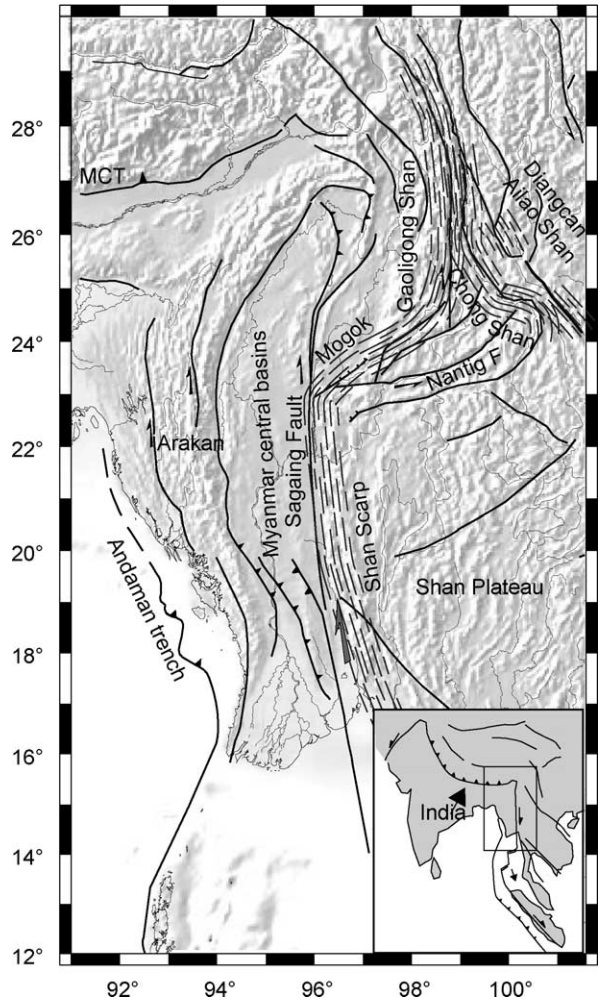

Fig. 1. Structural schema of Myanmar and western Yunnan (China) showing the main brittle structures and the metamorphic ranges. Inset is a simplified map of south-east Asia.

blocks. The Tertiary tectonic history of this region is a direct consequence of the India Eurasia collision. India has been moving northward for over 70 Ma. Final closure of the Neo-Thetyan ocean that separated the Indian craton from Eurasia probably occurred in the western Himalaya from 55 Ma (Garzanti et al., 1996) to 50 Ma (Searle, 1991). In central Himalaya and further to the east the beginning of continental convergence is poorly constrained and remains uncertain. However, the commonly proposed time for collision is 45+/−5 Ma. A similar age was deduced from the change in the relative motion between India and Eurasia.

2.2. Motion of India and intracontinental distribution of slip

Indian northward velocity decreased as it entered in collision phase with the Eurasian Plate to form the Himalayan range. The rate of the northward migration of the eastern syntaxis is not well constrained. However, if we accept that few shortening occurred between Siberia and South China, the northward migration of the Syntaxis should be of the same order to that of India. Present day relative motion of India with respect to Eurasia predicted by the global plate motion model NNR-Nuvel-1A (DeMets et al., 1994) is about 54 mm/yr oriented around N20°E. Recent geodetic determination of the convergence rate between India and Eurasia range from 47 mm/yr (Paul et al., 2001) to 40 mm/yr (Socquet et al., 2002b).

18 mm/yr of this convergence is absorbed by compressional deformation in the Himalayan arc (Molnar and Lyon-Caen, 1989; Bilham et al., 1997) while the remaining part is distributed in a large area spread from Tibet to Mongolia (Molnar and Tapponnier, 1975, 1977). In addition, the block along which eastern boundary of India is sliding is not stable Eurasia, but rather the Sundaland block (Simons et al., 1999; Michel et al., 2001). Taking this into account, the relative motion expected between India and Sundaland on the Myanmar boundary reduces to 35 mm/yr and rotates towards North at N7°E. Thus the Eastern Himalayan Syntaxis should move northward relative to Sunda at about 15+/−5 mm/yr and about 25 mm/yr relative to South China. Part of that motion must be accommodated in western Yunnan (Socquet et al., 2004).

2.3. Finite displacements

Paleomagnetic study of rocks from Tibet proposed 1700+/−600 km of crustal shortening and thickening of Eurasian crust north of India (Achache et al., 1984) since the collision. The corresponding penetration of India into Eurasia requires a comparable magnitude of right lateral shear across the area directly east of India (~2000 km compared to the 3400 km of northward motion of India over the same period). These relative displacements must be recorded in the geology of western Yunnan which lies between India, South China and Sundaland. Drainage basins pattern analysis showed that pervasive dextral shear strain of 6+/−1 throughout the 150 km wide region of the Three Rivers (Salween, Mekong and Yangtze rivers: Fig. 2) would account for ~1000 km of northward motion of India relative to South China while directly east of this region, another ~1000 km of northward motion is likely to have been accommodated by pervasive shearing through a westernmost zone of hundreds of kilometres wide (Hallet and Molnar, 2001).

2.4. Different tectonic interpretations for the regions east of the Indian indenter: review of geodynamic models

The region located east of the Indian indenter is important to understand the behaviour of the continental crust and thus has been the focus of numerous studies and models.

Comparison between analogue experiments in plasticine (Tapponnier and Molnar, 1977; Tapponnier et al., 1982) and geology have suggested that although most of the convergence was accommodated within the Himalayan

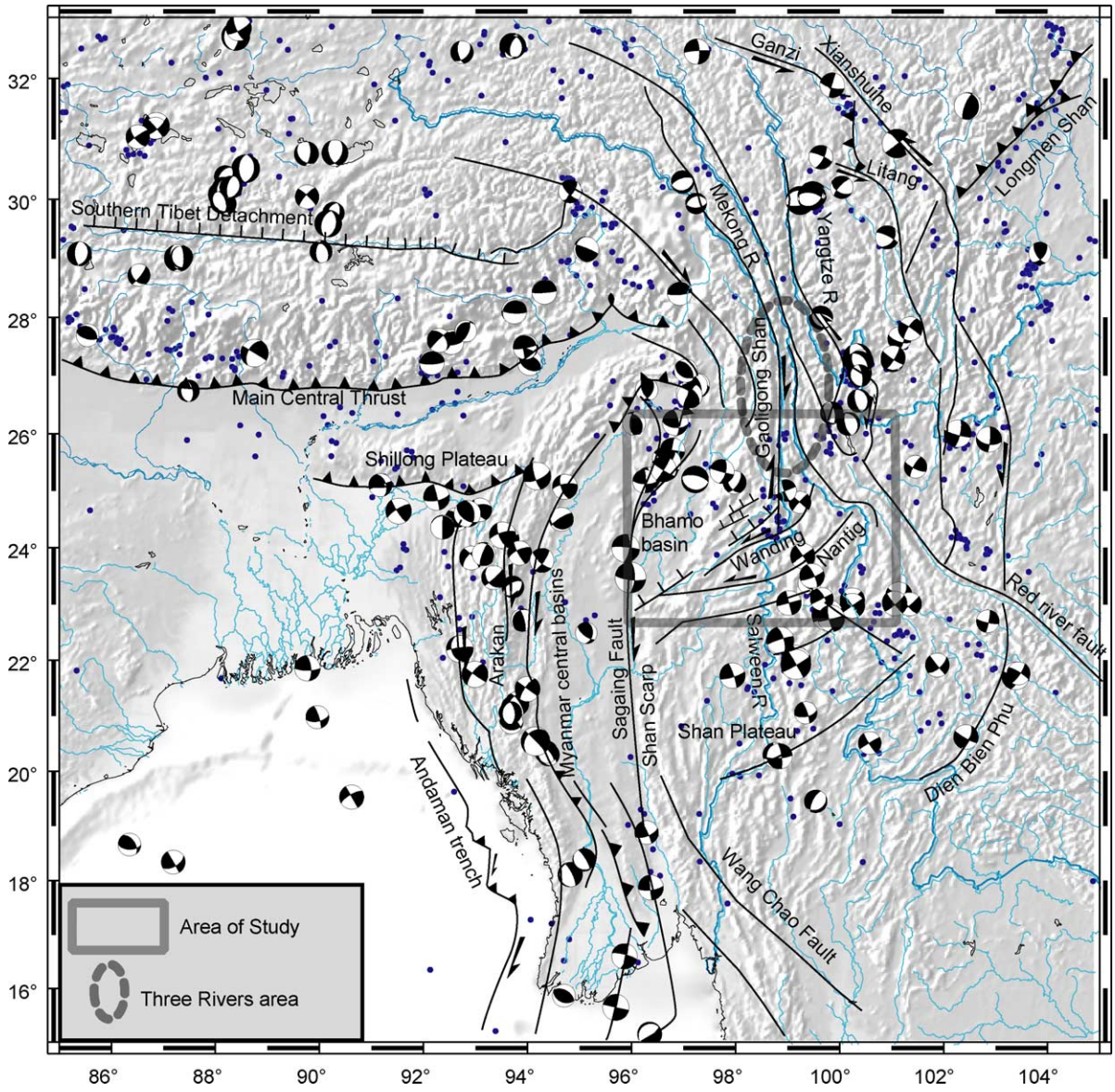

Fig. 2. Map of the active structures and seismicity around the Eastern Himalayan Syntaxis. Seismicity data from the Engdahl catalog.

range and into Eurasia, part of it being accommodated by several hundred kilometres of eastward displacement of two fragments of Eurasia: namely Indochina, and Eastern Tibet/South China. The extrusion of this second block is inferred to have reversed the displacement sense along the Red River fault zone.

In contrast, numerical modelling of a viscous Eurasia indented by a rigid India (England and McKenzie, 1982; England and Houseman, 1986; Houseman and England, 1986a,b, 1993; Houseman et al., 2001) show the growth of the Tibetan plateau by shortening and thickening of the Tibetan crust. The shortened area spreads eastward around the eastern corner of the Indian indenter. In the early models, (Tapponnier and Molnar, 1977; Tapponnier et al., 1982) no material was extruded eastward beyond the plateau. In the later models (Davy and Cobbold, 1991), eastward movement material beyond the Tibetan plateau was allowed on non-discrete faults as a continuous eastward bulge. The models show continuous clockwise rotational strain east of the north eastern edge of the Indian indenter, in western Yunnan.

Various authors (Dewey et al., 1989; Jolivet et al., 1990; Davy and Cobbold, 1991) suggested that the region east of India underwent a right lateral shear and large clockwise rotations within a broad north–south trending zone extending from southern Myanmar to the north of the Tibetan plateau. In accordance with some early models (England and Houseman, 1986) and in contrast to others (Tapponnier and Molnar, 1977), there is no eastward extrusion beyond the zone of right-lateral shear. All these models have different and geologically testable consequences for various time intervals.

Recently some models of the stress and strain patterns east of the Syntaxis attempted to incorporate geological

observations and some have been developed directly from earthquake and geodetic data (England and Houseman, 1986; Holt et al., 1991; Huchon et al., 1994; Holt et al., 1995). Because of the northward motion of the Syntaxis, the region has experienced rapid changes in the stress and strain pattern during the past 45 Ma of post-collisional convergence. Some authors (Huchon et al., 1994) have attempted to correlate some geological data with the predicted stress fields through the period of post-collisional convergence throughout a continuous motion between the plates. Others (Holt et al., 1991, 1995) have derived the present stress strain and velocity field from earthquake data considering that the seismicity is representative of the total strain. These models regard the deformation in the Eastern Himalayan Syntaxis region as a continuum and show that stress trajectories diverge eastward away from the Syntaxis: the pattern is helicoïdal with a 180° rotation of the maximum horizontal stress, from north–south in the Himalayan arc to east–west in Western Sichuan and South China and finally to north–south in Myanmar and Indochina.

Geological studies, mainly based on mapping of recent structures and microtectonic analysis, in Sichuan and western Yunnan (Ratschbacher et al., 1996; Wang and Burchfiel, 1997; Wang et al., 1998; Wang and Burchfiel, 2000) allowed to test the models and showed that the clockwise flow around the syntaxis was accommodated at the surface by large curved strike-slip faults individualizing crustal fragments. Deformation within blocks is minor and the boundaries are characterized by distinct fault kinematics and pattern of stress. However, all indicate relatively intense deformation near the corner of the indenter. The deformation field radiates around the Syntaxis. For regions initially situated north of the Eastern Himalayan Syntaxis, this deformation is likely to comprise two main phases: a phase of pure shortening oriented roughly northeast–southwest, followed by right-lateral shear once the deforming region has been advected past the syntaxis (Wang and Burchfiel, 2000).

2.5. Significance of a comparison between ductile and brittle motions

The flow around the Eastern Himalayan syntaxis described in the different models is continuous, represented by a viscous layer. However, geological observations showed that, at the surface, the motion is distributed along brittle faults highlighting low deformable blocks and rule out the hypothesis of a continuous bulge. This deformation can be explored using motion on active faults, seismicity and Global Positioning System (GPS) (Holt et al., 1995; Chen et al., 2000; Wang et al., 2001). Deformation in the lower crust can be approximated as a viscous flow because of its ductile rheology, the localisation of the deformation occurring only in the shallow part of the crust. Therefore, one may wonder about the link between lower and upper crust: is the shallow velocity field indicative of the one at depth? Does it make sense to compare the velocity field obtained from GPS and the stretching direction in the lower crust? Another issue that concerns is the stretching lineations: can we regard the exhumed ductile lineations as characteristic of the tectonic motion as it was 20 Ma ago? Can we access by this way to the evolution of the tectonic style of the Eastern Himalayan syntaxis?

An attempt of such a comparison has been performed in the Aegean region: the strain pattern shown by exhumed metamorphic complexes in the whole region and the present strain pattern as documented by GPS measurement are very similar (Jolivet, 2001). The author concludes that rates of motion cannot be extrapolated in the past although strain patterns may not. This implies that fossil ductile strain pattern versus the active one inferred by GPS must be compared to explore the evolution of the deformation mode. Post-exhumation rotations undergone by the rocks and shown by paleomagnetic data must be integrated, especially in tectonic regions where shear and lateral motion are important.

3. Analytical method

We have carried out detailed mapping of the geometry of the structures based on interpretation of Landsat 7 imagery. Stream, valleys, bedding trends can be interpreted as faults, folds, schistosity or even stretching lineation. Such imagery analysis allowed us to highlight the structural relationship between faults in complex areas and to perform a continuous mapping of ductile stretching direction where the basement crops out by interpolation of field observations and measurements.

In the field, we have characterized the geometry of stretching direction by orientation analysis of deformation structures. Foliations and stretching lineations were used to determine the orientations of the principal strain axes. We made use of rolling structures, S-C shear bands, pressures shadows as kinematic indicators in rocks deformed in ductile conditions.

In addition, we used meso-scale fault-slip data collected along main faults, including fault size and attitudes, slicken-slides orientation to determine sense of slip. We used the following method to derive principal strain axis orientation and ratio. The inversion resolves the mean state of stress from a population of striated faults measured in the field. Measurements were performed in rocks of various ages. The inversion process is described extensively by Careygailhardis and Mercier (1987). The algorithm first defines compressional and extensional zones resulting from superimposition on compressional and tensional quadrant defined by the two nodal planes, and thus enables us to test the data homogeneity. This also restricts the space where the principal stress axes must be searched. Then for each principal stress reference within the confined zone, the R value $(\sigma 2-\sigma 1)/(\sigma 3-\sigma 1)$ is computed.

4. Geodynamic setting and structures

4.1. West Sunda

The relative motion between Australia and Sunda implies a variation of the obliquity of the subduction increasing from the south along the Java trench to the north in Sumatra. Toward the north, the Sunda trench is followed by the Andaman trench, and the Great Sumatra Fault is relayed by the Sagaing fault north of the Andaman Sea pull-apart. The Andaman trench is separated from the Sunda trench by the 90° E ridge, limiting India and Australia plates. East of this trench, the Arakan accretionnary wedge is affected by large N/S strike-slip faults (Fig. 1) (Socquet et al., 2002a). This mountain belt is bounded by the Myanmar Central Basin, of the Eocene age, which have been inverted in the Late Miocene (Rangin et al., 1999). The Sagaing fault cuts through the basins and presently ends up into an extensional horse tail, both toward the south, in the Andaman pull-apart basin, and toward the north. The Mogok metamorphic belt is exposed along the N-trending Shan Scarp. Deformation is ductile and shows right-lateral wrenching almost parallel to the Sagaing fault. In central Myanmar, the Shan Scarp is affected by a high grade metamorphism of the Oligocene to lower Miocene age, caused by a NNW-SSE ductile extension associated with crustal thinning (Bertrand et al., 1999). Further north, the Shan Scarp connects the Mogok metamorphic belt, where gneiss and ruby-bearing marbles crop out. This NE-trending belt continues in western Yunnan and along the eastern flank of the Bhamo Basin.

South of the Syntaxis many Eocene to Miocene shelf basins were opened in Thailand (Huchon et al., 1994; Rangin et al., 1999; Morley, 2001; Morley et al., 2001; Morley, 2002) as a result of the oblique convergence between India and Sunda.

4.2. Western Yunnan

In western Yunnan, the tectonic features are influenced by both the Eastern Himalayan Syntaxis system and the northern termination of the Sagaing fault. Deformation is thus distributed between strike-slip and normal faulting (Fig. 1). Active left-lateral slip along NE trending strikes is evidenced by seismicity; stream offset analyse indicate that

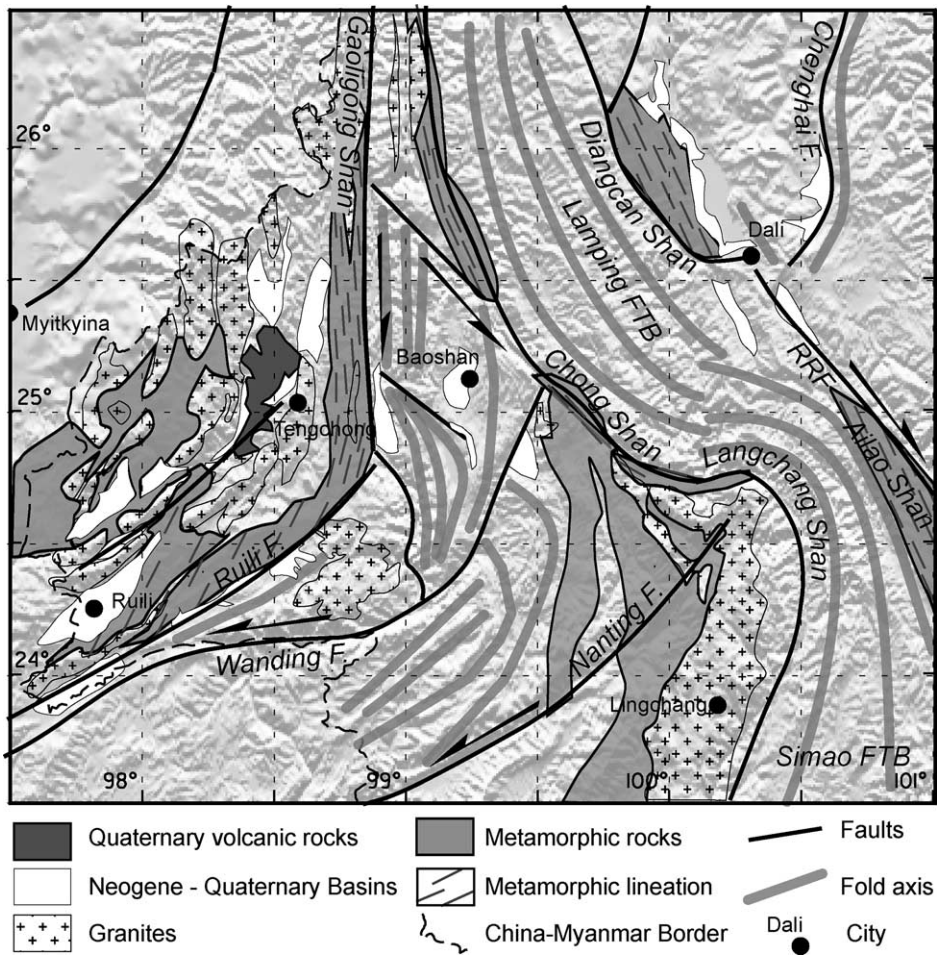

Fig. 3. Simplified geological map of western Yunnan (China).

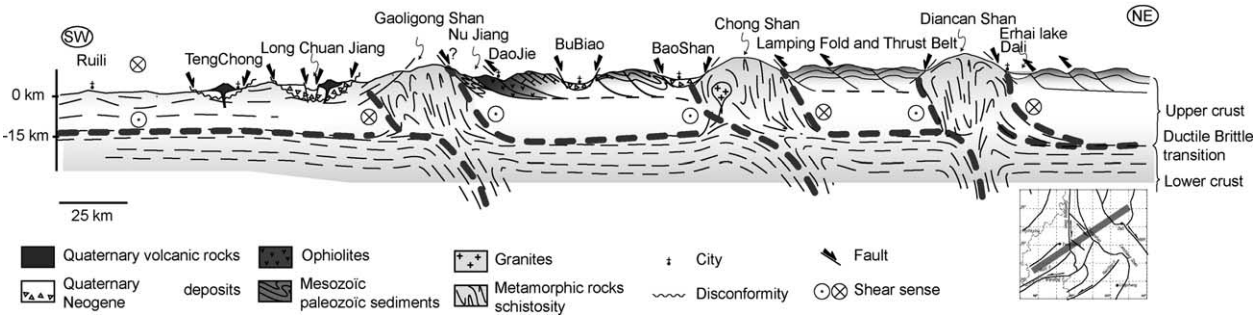

Fig. 4. NE–SW interpretative cross section of western Yunnan.

these faults (Nanting, Wanding faults) may accommodate 1 mm/yr (Lacassin et al., 1998). Fig. 3 is a simplified geological map of western Yunnan and Fig. 4 is an interpretative schematic cross section showing the vertical relationship between the different units. Western Yunnan is crossed by three shear zones characterized by high mountain belts mainly composed of high grade metamorphics and mylonitic rocks, and affected by active faulting.

The easternmost metamorphic range, the Gaoligong Shan composed of verticalized foliated granites and mylonites is flattened westward and joins the Mogok metamorphic belt in Myanmar. East of the Gaoligong Shan lie the Chong Shan metamorphic range and the Diangcan Shan, the North western continuity of the Ailao Shan, which presents a vertical shistosity and a left-lateral motion. These three metamorphic ranges are separated by sedimentary fold and thrust belts in the east and by volcanics and Quaternary basins west of the Gaoligong as illustrated by Figs. 3 and 4. To the north these structures converge and are pinched into the inner part of the Eastern Himalayan Syntaxis.

4.3. Eastern Himalayan syntaxis

The syntaxis features, shown in the Fig. 2, are characterized by a set of curved faults around the north eastern edge of the Indian indenter which distributes the displacement during the clockwise rotation of crustal blocks (Figs. 1 and 2). The three main active fault systems are: (1) the convex northeast left lateral Xianshuihe-Xiaojiang, which is known in Tibet as the Ganzi fault and somehow connected in Indochina with the Dien Bien Phu fault, (2) the north–west trending Red River Fault and (3) the north–east trending complex of left-lateral and normal Dali faults system continuing southward as the Wanding-Nanting faults (Wang et al., 1998).

The Eastern Himalayan syntaxis is an active and seismic region. Fig. 2 shows that the seismicity is penetrative. The Dali fault system is characterized by a diffuse seismicity with left-lateral and extensional motion along a NE-trending faults. The average tension axis is E–W. Activity is also present in the Lamping fold-and-thrust-belt. Some events are reported along the Nanting fault, where historic earthquakes with SE trending tension axis are observed (Holt et al., 1991). Seismic activity is present along the Gaoligong Shan and its southern continuation characterized by the Ruili fault system. An earthquake swarm occurred in the southern part of the fault in 1976 ($M = 5.29$–7.1) (Holt et al., 1991). The earthquakes have been interpreted as related to left-lateral movement along NE-trending faults. Further to the east, at the limit between the Ruili fault system and the Bhamo basin in Myanmar (Fig. 2), right-lateral shear along N-trending strike and normal focal mechanisms are reported. The Sagaing fault is expressed by many right-lateral focal mechanisms, particularly in its northern termination.

5. Regional analysis

The present study focuses on western Yunnan and explores the relationships between the Sagaing fault and the Red River Fault, south of the Eastern Himalayan Syntaxis (Figs. 1 and 2) and previous ductile deformation. We will describe structures, from east to west, in several key areas.

5.1. Dali fault zone and Diangcan Shan

The Dali fault system is constituted by a set of north–south left-lateral faults cutting through folded Paleozoic and Triassic rocks (Fig. 5A). It is bounded to the west by the north-northeast-trending Jianchuan fault which is the termination of the northwest-trending left-lateral Zhongdian fault. The eastern boundary of the fault zone is the north-trending Chenghai fault zone, and the northern boundary is the Daju fault. These left-lateral faults strike toward the south and abut the Ailao and Diangcan ranges.

These faults delineate blocks which have suffered older deformation that condition the young faults. Therefore, crustal anisotropy may have played an important role in the localisation of the faults.

We have carried out a detailed mapping of the southern termination of the Chenghai fault and its relationship with the Red River Fault and the Ailao and Diangcan metamorphic ranges based on Landsat 7 imagery (Fig. 5B

colour print) interpretation and field work. The tectonic interpretation is illustrated by the Fig. 5B.

Many basins were opened along the faults, most of which are Quaternary in age (Wang et al., 1998). This indicates that this fault system is recent, or active.

The Ailao Shan shear zone continues toward the NE in the Diangcan Shan, which is offset left-laterally about 20 km to the southwest in the Dali area. The relationship between these metamorphic ranges and the recent Dali fault system is not clear.

5.1.1. Diangcan Shan shear zone

The Diangcan Shan shear zone separates the Dali fault system from the Lamping-Simao fold-and-thrust-belt. The Ailao Shan shear zone was active as left-lateral from ~35 to 17 Ma, and the Red River fault which partly reactivated the Ailao Shan shear zone, has been active as right-lateral fault since ~4 Ma (Leloup et al., 1995). Recent motion on this fault has been estimated around 5 mm/yr from stream offset analysis (Replumaz et al., 2001). Rocks of the Diangcan Shan record at least two periods of exhumation at ~20 Ma and from ~4 Ma to present (Leloup et al., 1993). The ductile deformation associated with the older period of exhumation is characterized by a vertical schistosity and a left-lateral motion in the central part of the range. However, south of the Diangcan Shan, we observe a flat or folded foliation, marked by a N120° lineation. S-C shear bands, rolling structures on feldspar and pressure shadows around garnet porphyroclasts indicate a top to the southwest shear. The presence of boudinage and sheets folds (Fig. 5E) characterizes intense stretching. In its southern part the Diangcan Shan may be affected by an extensional shear band, a detachment, which separates high-grade metamorphics from low-grade metamorphic sedimentary rocks (Mesozoic) on the top, which are exposed south of the Diangcan Shan (BGMRY, 1983). This detachment fault would have been reactivated later by a brittle vertical fault with a left-lateral transtensile motion, as described previously.

The Diangcan Shan is affected on its east side by normal faults (Fig. 5E) cutting through the foliation and thus participating the late exhumation of the metamorphic core. These faults have been interpreted as the offset continuation of the Red River Fault (Leloup et al., 1993), however, their characteristics are more those of a detachment fault because of their normal component rather than a right-lateral slip (Wang et al., 1998). The northwestern continuity of the active Red River Fault and its interaction with the Dali fault system is uncertain.

5.1.2. Termination of the Chenghai fault

The Red River fault and the Chenghai fault merge west of the Minbu basin (Fig. 5B). Stream deflections show active left-slip along Chenghai fault (Wang et al., 1998). Geometry of the Minbu basin is consistent with a right lateral pull-apart along the Red River Fault. The northwestern border of the basin is the end of the Chenghai fault that limits the Quaternary deposits from the Devonian and Cretaceous rocks. The Devonian rocks are folded and probably thrust over the westernmost Cretaceous rocks by a curvilinear fault. This fault continues further to the northwest and shows a clear geometry of right-lateral strike-slip fault underlined by small pull-apart basins as shown on Fig. 5C. This fault then enters the Erhai basin and further the eastern coast of the Erhai Lake. It might represent the continuation of the Red River fault.

East of the Erhai Lake, Paleozoïc rocks are involved into a broad N140° anticline (Fig. 5D). A northwest trending Quaternary basin lies unconformably on the folded Permian ophiolites. This basin is in turn controlled by fault morphology (Fig. 5D and E) with triangular facets compatible with a normal motion. To the north, a granitic pluton is exhumed and pinched along an east–west trending direction.

The general geometry of this area can be described as a set of triangular blocks separated by faults along which the Quaternary basins have opened. The blocks are entirely deformed by folding and seem to have slipped against northeast-trending left-lateral fault of the Chenghai fault

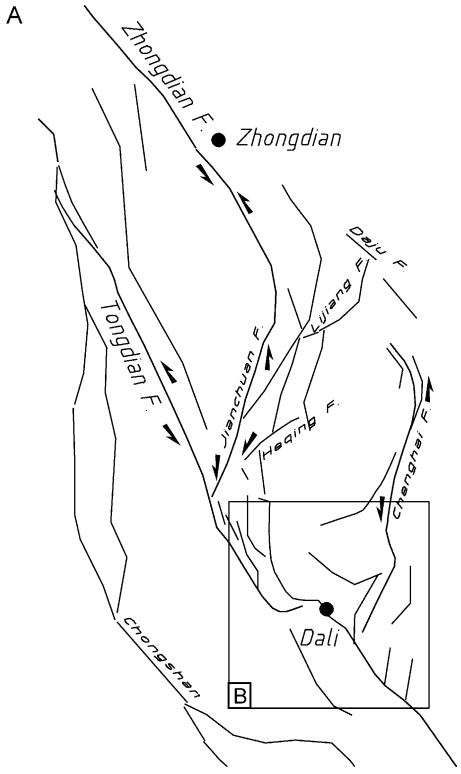

Fig. 5. (A) Structural map of the Dali Fault Zone. (B) Geology and structures of Dali area from Landsat 7 imagery interpretation (the zone is located on A). (C) Geometry of the northern termination of the Red River fault from Landsat 7 imagery interpretation (location on B). (D) SW–NE cross section east of the Diangcan range (location on B). (E) Photographs taken along the cross section D. Mega-shear-band (1) and sheet-fold (2) in the Diangcan Shan. Fault Gouge (3) and normal fault plane (4) along the Diangcan Shan NE side. Thrust fault (5) east of Erhai lake and triangular facets attesting the active morphology of a normal fault-bounded basin (6).

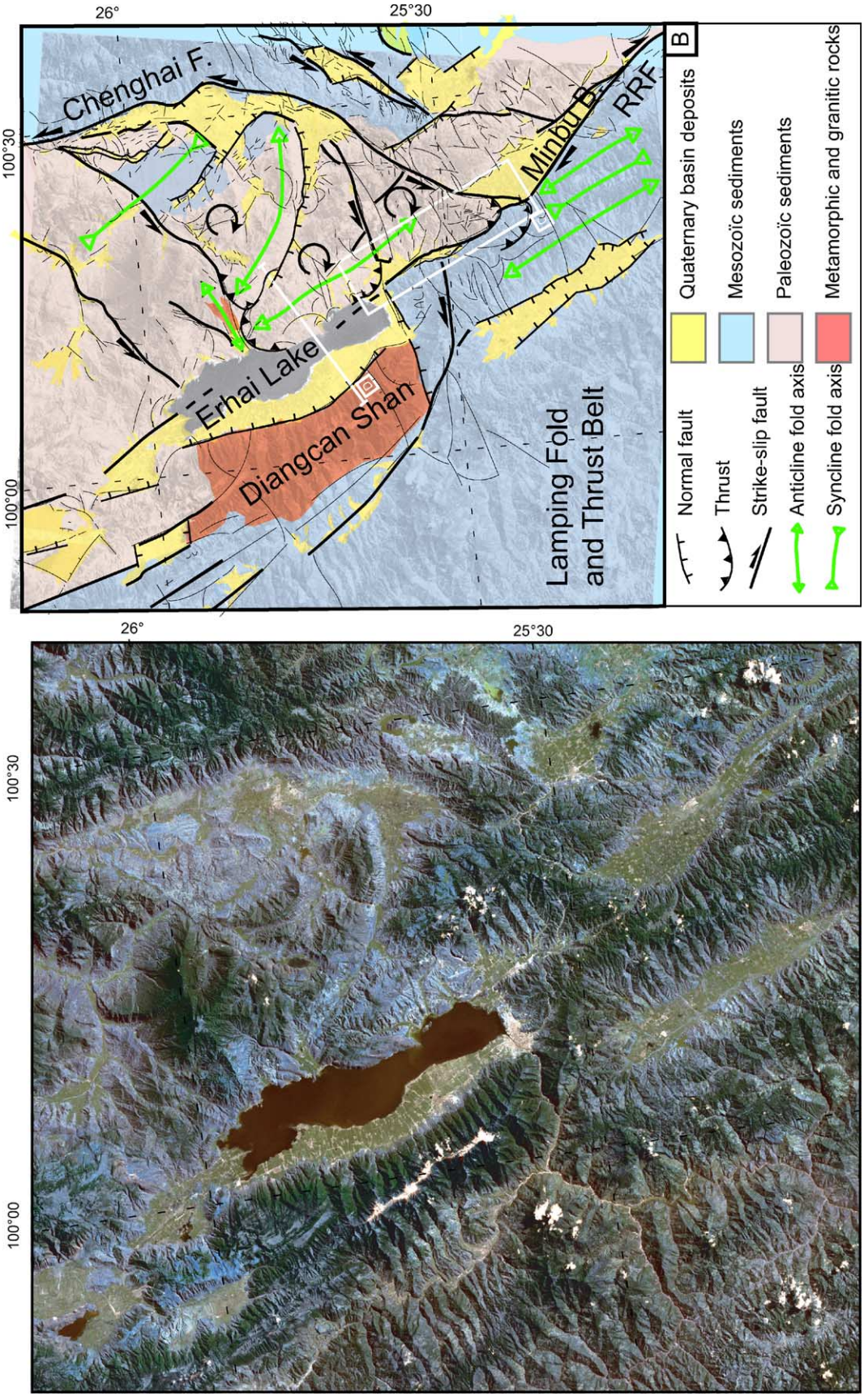

Fig. 5. (*Continued*)

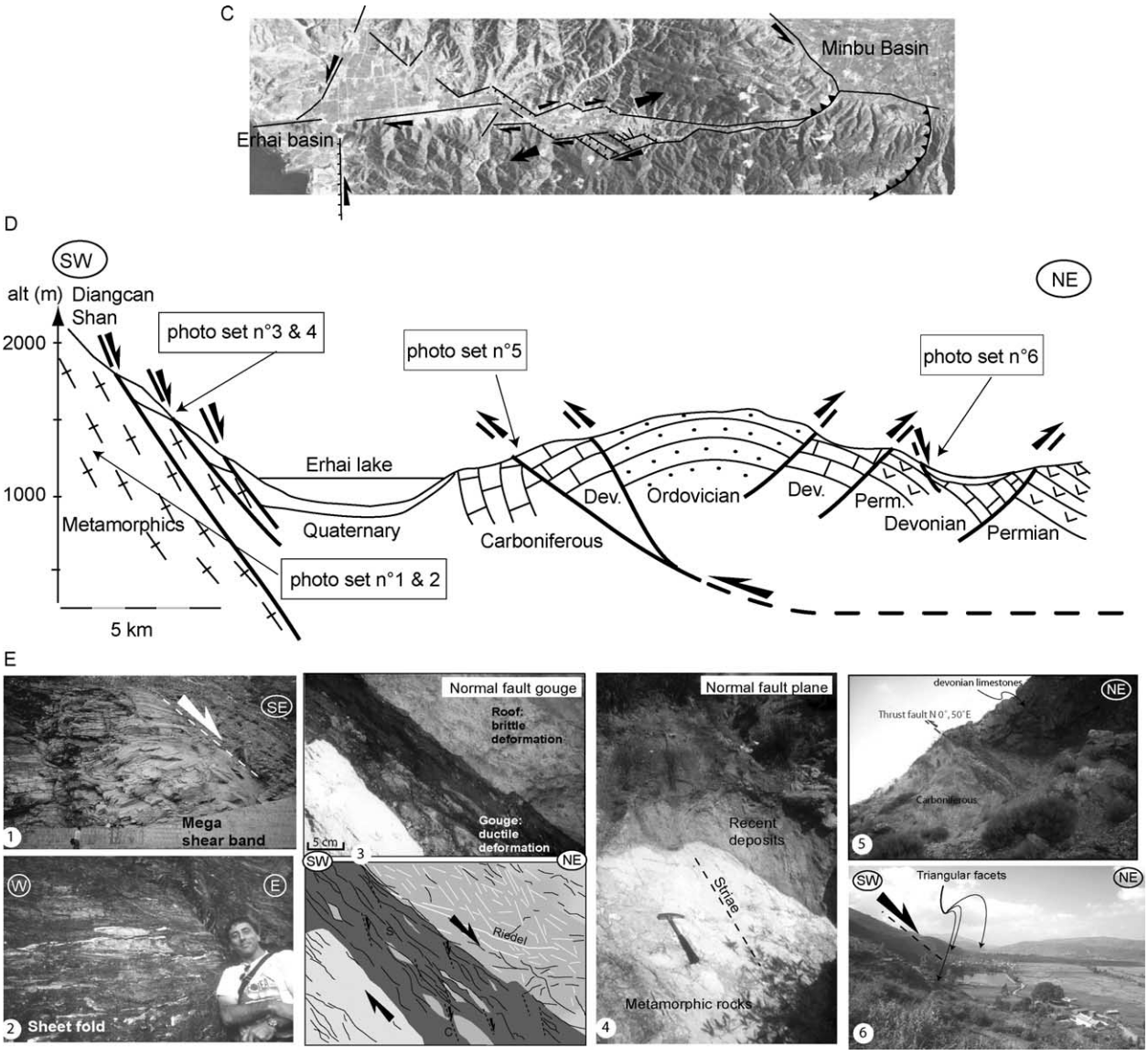

Fig. 5. (*Continued*)

zone. The motion is accommodated by compression inside the block (folding), thrusting and normal faulting at the advancing and receding sides perpendicular to the motion. This geometry can be interpreted as small size (10–20 km) crustal blocks moving along the termination of the left-lateral Chenghai fault in addition to the rotation of larger blocks (Wang et al., 1998). The blocks are affected by a clockwise rotation and abut the Red River fault system and the Diangcan Shan. We propose that the late Neogene evolution of this area is marked by block impingement of the Red River fault/Diangcan metamorphics and rotation of blocks due to right-lateral motion along the termination of the Red River fault system. The contrast between the Chenghai Fault System and the set of strike-slip faults affecting the Lamping fold-and-thrust-belt suggest that the metamorphic belt actually behaved as a buffer zone which accommodates an important part of horizontal motion. An analogy can be made with the termination of the Xianshuihe fault system in the Kunming region and the bending of the Red River fault due to its indentation by the Xianshuihe fault system (Wang et al., 1998).

5.2. Lamping fold and thrust belt

The Lamping Simao fold and thrust belt is bounded by two high metamorphic ranges: the Diangcan/Ailao Shan in the east and the Chong/Lanchang Shan in the west as shown on Fig. 3. The belt is mainly constituted of non-marine redbeds of the Jurassic to Early Cenozoic age (BGMRY, 1990). The redbeds overlie the Triassic volcanic rocks and Paleozoic sediments exposed along boundaries of the belt. Rocks have been shortened in a NE–SW direction. Folding began in the Eocene and was completed by the Pliocene (Wang and Burchfiel, 1997). The folds and the thrusts form an arcuate pattern convex to the southwest in the Lamping area. This pattern is relayed in the south by a narrow convex

to the northeast area, the Wuliang Shan. Wang and Burchfiel (1997) have shown that the Lamping Simao element was first deformed along and NW trend and that the Wuliang arcuate trend was superimposed later. Paleomagnetic study show important clockwise rotations within the fold and thrust belt (Sato et al., 2001).

The Lamping Fold-and-Thrust-Belt is situated in front of the Dali fault system which abuts the Ailao Shan. The same geometry can be described in the south where the arcuate Simao Fold-and-Thrust-Belt is situated in front of the curved part of the Red River Fault, indented by the termination of the Xianshuihe fault.

5.3. Chong/Lanchang Shan

The northwest–southeast trending Chong Shan separates the Lamping Fold-and-Thrust-Belt from the Baoshan area.

The Chong Shan is a belt of mylonitic rocks, generally mapped as the Precambrian (BGMRY, 1983) although the mylonitization is Middle to Late Cenozoic in age (Wang and Burchfiel, 1997). In its central part, the metamorphic range is offset left-laterally. North of this offset the metamorphic range is referred to as Chong Shan, and south of it, as Lanchang Shan.

A schematic cross section of the Chong/Lanchang metamorphic belt is illustrated by the Fig. 6. Metamorphic rocks are overthrusted by pelitic sediments of the Lamping Fold-and-Thrust-Belt. The core of the range is mainly composed of mylonite, high temperature gneisses, and foliated granites. Laterally strongly deformed Precambrian (BGMRY, 1983) metasediments are exposed, as shown by the sheet folds of the picture 6B (a). These metasediments are pinched against the mylonitic rocks of the core of the range, although their structural relationship is not clear. To the south, these metamorphic sediments extend in a belt of

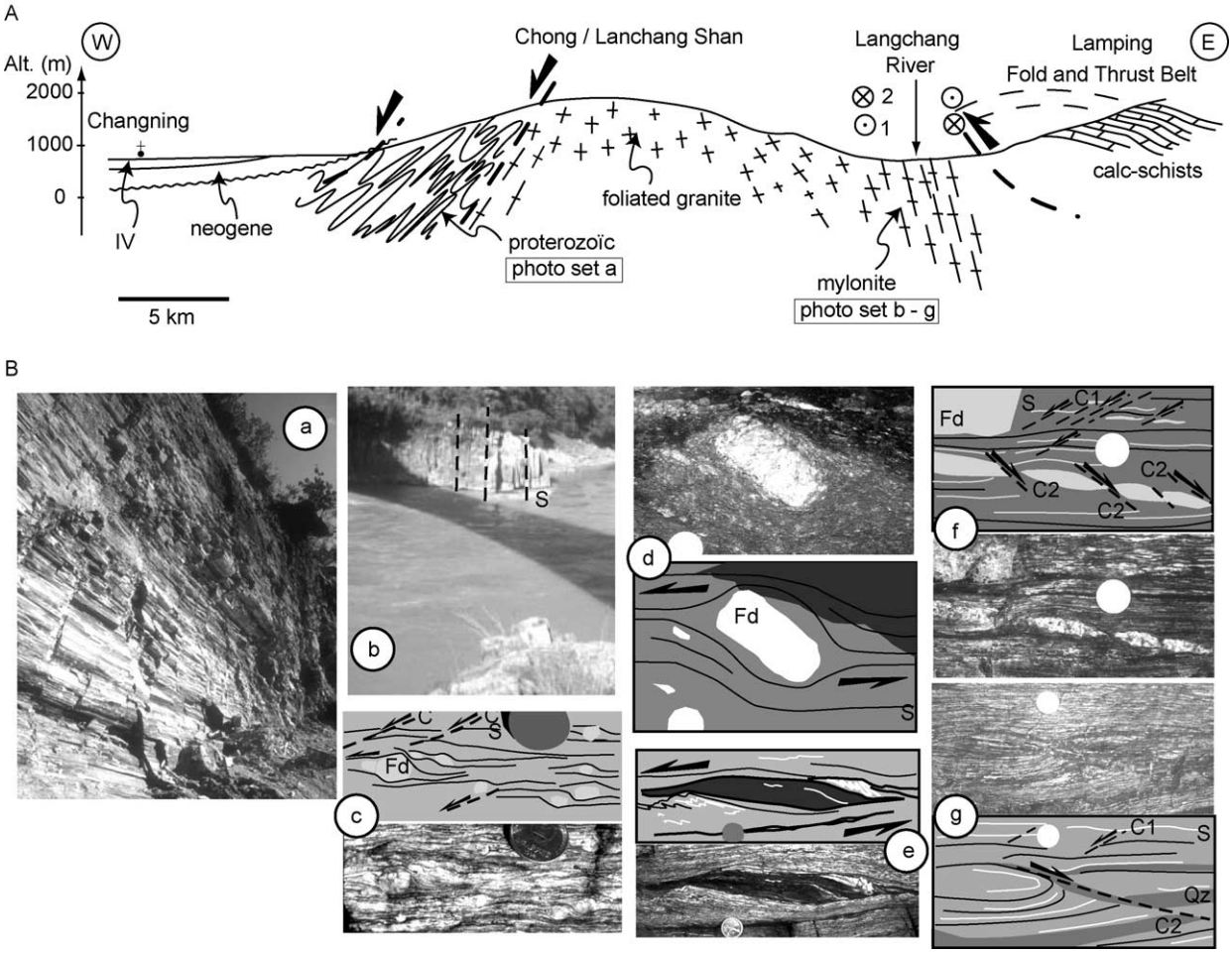

Fig. 6. (A) Schematic E–W cross section of the Chong/Langchang Shan metamorphic range and ductile deformation. (B) Photographs of ductile deformation in the Chong/Langchang Shan (cross section A). (a) Sheet-folds of N175° axis in Proterozoïc metamorphic sediments of the Langchang Shan. (b) Vertical schistosity of the mylonite along the Langchang River. (c) CS shear bands and pressure shadows in a gneiss showing left-lateral ductile shear. (d) Magmatic feldspar relic left-laterally sheared. (e) Asymmetric vein (mainly composed of biotite and overturned folds toward the NW in the schistosity) indicating a left-lateral ductile shear. (f) Left-lateral ductile SC shear bands overprinted by right-lateral ductile-brittle shear characterized by asymmetric boudinage of quartz vein. (g) Ductile left-lateral SC shear bands and right-lateral later boudinage.

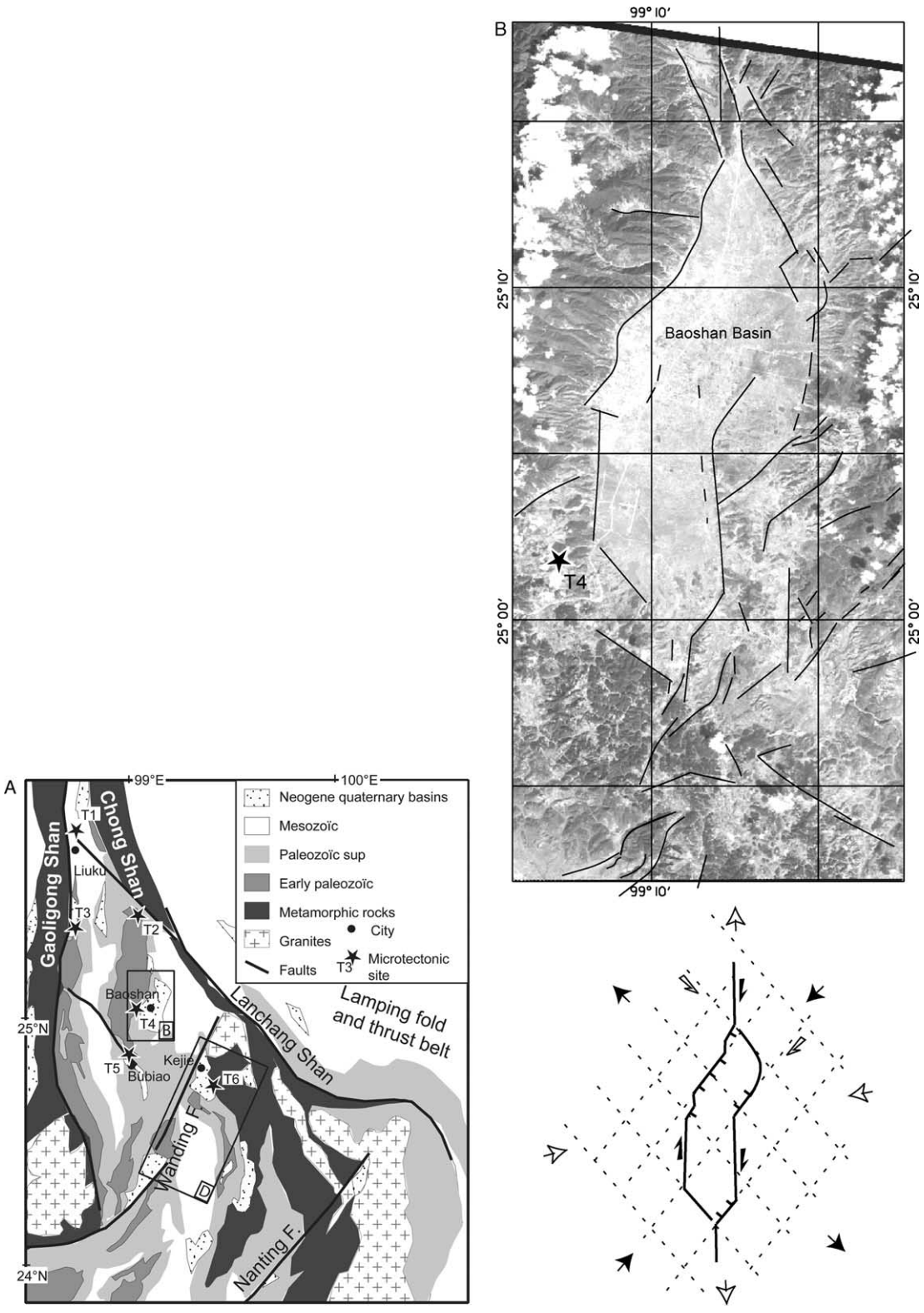

Fig. 7. (A) Simplified geologic and structural map of the Baoshan area, bounded by the Gaoligong Shan in the west, the Chong Shan in the East and the Wanding fault in the South East. (B) Geometry of the Baoshan Basin from Landsat 7 imagery (Zone is located on A). Schematic tectonic interpretation for the opening of the Baoshan basin is also given. (C) Fault slip analysis diagrams located by stars in the interpretative maps A, B, D and 8. Diagrams are lower hemisphere. Faults are drawn as great circles and striations as arrows. Two tectonic phases are individualized in many site. The early one, NNW extension associated with ENE compression, affect Paleogene sediments, while NNE compression and ESE extension is in Neogene basin deposits. (D) Geometry of the north-eastern part of the Wanding fault and mapping of Kejie basin recent deposits from Landsat 7 imagery and field observations (Zone is located on A).

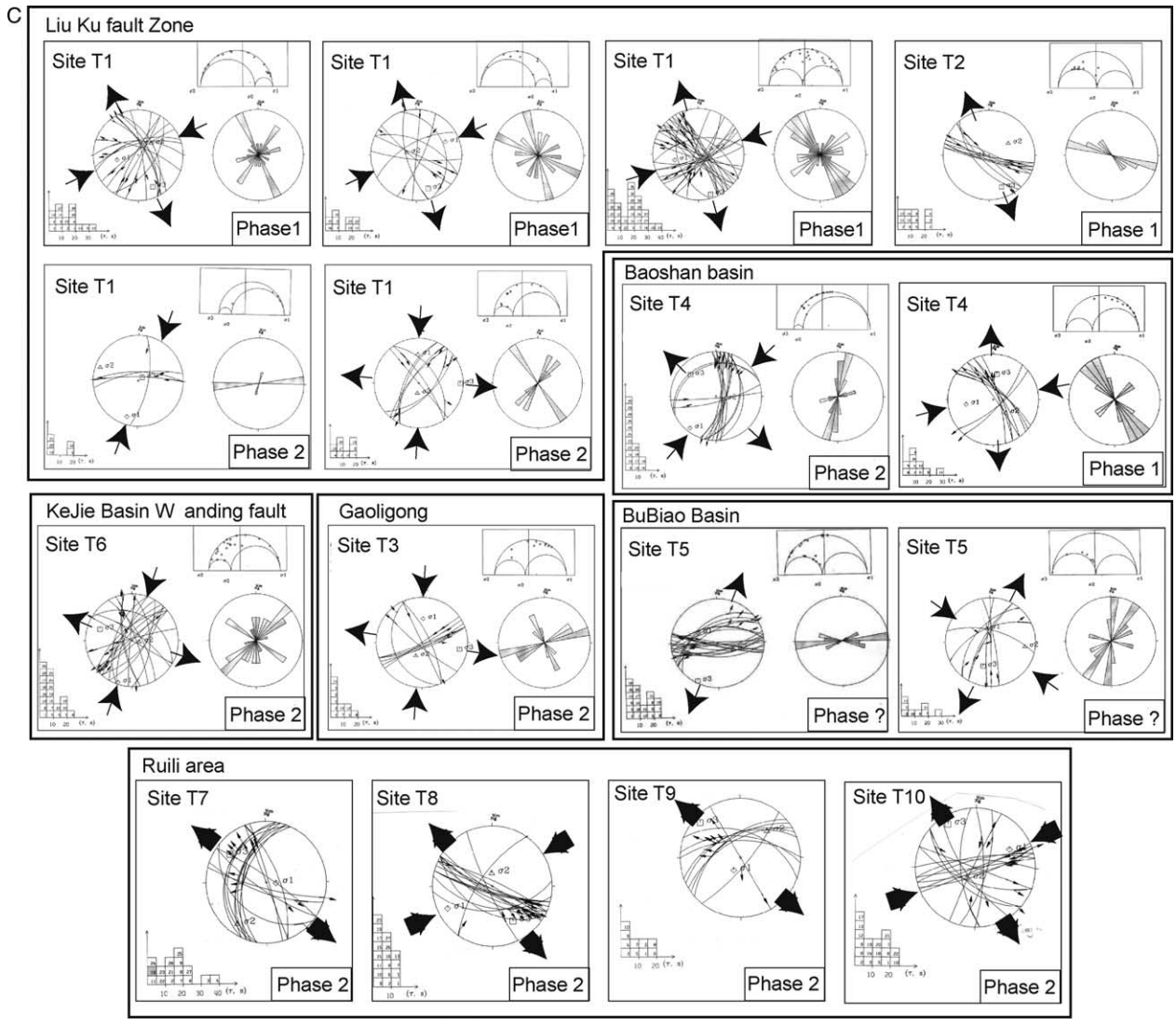

Fig. 7. (*Continued*)

high-grade precambrian metamorphic rocks and large granitic plutons (BGMRY, 1983). They are separated by the ophiolite and the blue-schist-bearing Changning suture (Metcalfe, 1996) from a belt of the Paleozoic sedimentary and low-grade metamorphic rocks, east of the suture.

In the field, the schistosity ranges from sub-horizontal to sub-vertical as illustrated by the picture 6B (b). Mineral stretching lineation fluctuates around an average N140° direction. Interpreted stretching lineations from Landsat 7 imagery show that directions roughly follow the trending direction of the metamorphic range. The study of ductile deformation criteria, S-C shear bands (Fig. 6B(c)), pressure shadow (Fig. 6B(c) and (d)), rolling structures, ductile overturned folding (Fig. 6B(e)), indicate left-lateral ductile shear whatever the dip sense of the foliation. This implies that the Chong/Lanchang Shan was a left-lateral ductile shear zone. Moreover, the Changning ophiolitic suture is truncated by the Chong Shan and almost certainly continues northwards as the Lancangjiang suture (Metcalfe et al., 1999) implying a total left-lateral offset of 250 km. The mylonitisation being Middle to Late Cenozoic, the Chong/Lanchang Shan is comparable to the Ailao Shan. Those two left-lateral shear zones have probably been active simultaneously.

This ductile deformation is superimposed by a second deformation phase at the ductile brittle transition. This second phase is marked by boudinage (Fig. 6B(f) and (g)), crystallization of quartz veins and late right-lateral shearing of those veins (Fig. 6B(f) and (g)). This second deformation phase affecting the Chong/Lanchang Shan may be interpreted as a right-lateral drag by the Gaoligong shear Zone.

5.4. Baoshan area

The triangular block (Baoshan tectonic element) (Wang et al., 1998) situated between the Gaoligong Shan, the Chong Shan and the Wanding fault, is composed of folded Paleozoïc to Mesozoïc sediments faulted and overlain by

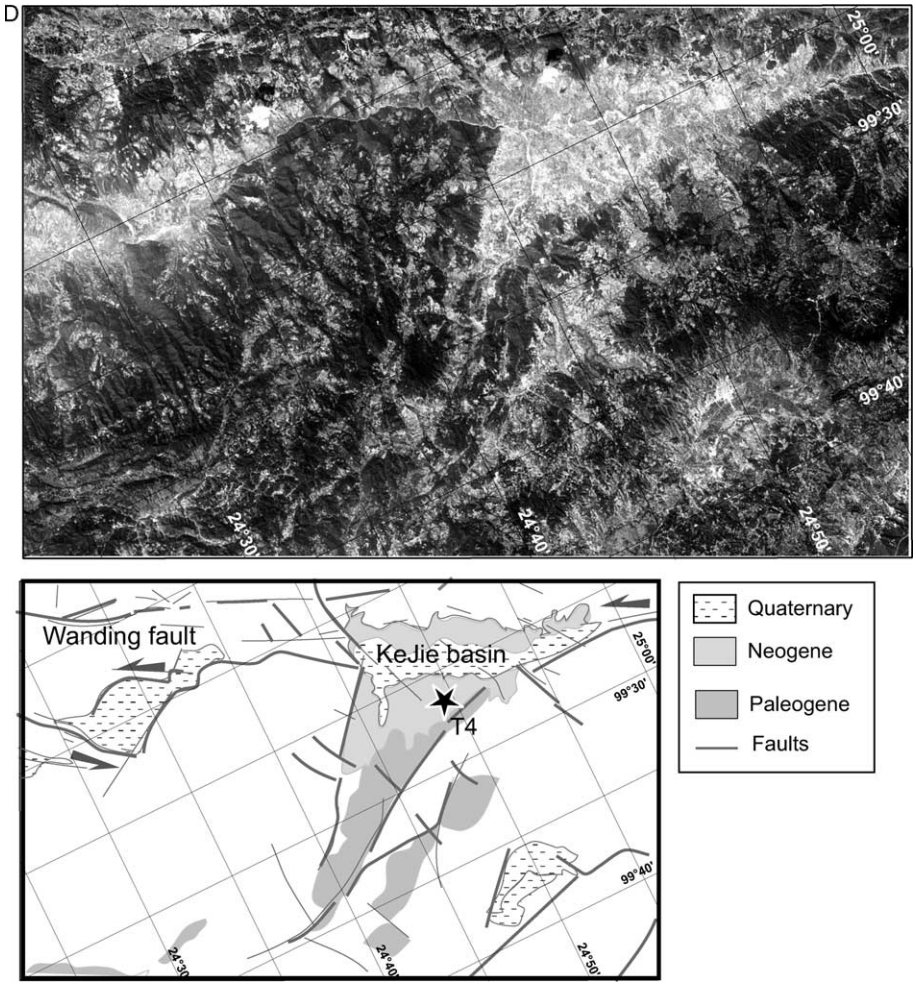

Fig. 7. (*Continued*)

Quaternary basin deposits (Fig. 7A). In this area, two regions are characterized by different tectonic patterns.

5.4.1. Liu Ku fault zone

The northern one is diamond-shaped and contains the Baoshan Quaternary basin (Fig. 7A). The bedding presents a general N/S direction. To the north, south of Liu Ku (Fig. 7A, site T1), the rocks are affected by a set of NW trending brittle faults, called hereafter Liu Ku fault zone. This fault zone offsets left-laterally the Chong Shan metamorphic range in its central part. Fault slip analysis shows a N150° trending preferential direction of left-lateral faults and the conjugated N60° right-lateral transtensive faults. This fault pattern is compatible with ENE compression associated to a NNW extension (Fig. 7C: phase 1). The age of this left-lateral brittle motion is poorly constrained because it affects upper Paleozoic to early Mesozoic age rocks only. A second state of stress has been individualized on the same sites (Fig. 7A, site T1), showing an anticlockwise rotation of the stress tensor of 45° (Fig. 7C: phase 2). Southeast of Liu Ku (Fig. 7A, site T2), where the brittle fault system offsets the Chong Shan, fracturation analysis shows a preferential ESE direction of faulting associated with a left-lateral motion. This is consistent with the early state of stress described in the Liu Ku area.

To the west, the region is bounded by the Gaoligong Shan where the rocks are affected by N–S right-lateral faults associated with ENE left-lateral faults (Fig. 7A, site T3). This implies a NNE compression and an ESE extension, which is consistent with the second state of stress described in the Liu Ku area.

5.4.2. Baoshan basin

The bean-shaped Baoshan (Fig. 7B) basin underwent a polyphased history which is indicated by a different morphology in its northern and the southern parts. The northern part of the basin is a regular rhomb-shaped basin and the southern part is aligned N–S. The western side of the basin shows a remarkable morphology showing drainage

cutting deeply the slope and indicating a recent uplift. This suggests recent NW–SE extensional component. Fault-slip data analyses (Fig. 7A, site T4) indicate that the basin has been affected by a set of left-lateral transtensile faults with a NW/SE direction conjugated with NE-trending right-lateral faults. This state of stress is referred as 'phase 1' is compatible with the Liu Ku fault system previously described. This state of stress cannot account for the extension and the formation of the basin, but is nevertheless associated with an earlier dislocation of the platform. The basin has been affected by at least a second state of stress 'phase 2' with NNE-SSW compression and NW–SE extension. We also observed sub-vertical N/S right-lateral faulting which are compatible with the same state of stress. This direction characterizes the southern part of the Baoshan basin. N–S faults are conjugated with ENE left-lateral faults. We therefore think that the S2 stage is a combination of the right-lateral pull-apart opening of the Baoshan due to the proximity of the Gaoligong fault system. The faults reactivate an earlier NW and SE conjugate fault system with E–W compression.

5.4.3. Bubiao area

The southern region presents a triangular shape (Fig. 7) and shows different tectonic features. Folds and thrusts are arcuated convex to the northeast. The bedding pattern is fan-shaped in the north and south extremities of the region. The crescent-shaped Bu Biao basin belongs to this southern tectonic region, and seems to have been bent after its opening. This suggests that the arcuate pattern is recent at least locally and probably throughout much of the complex. Microtectonic measurements bounding the basin (Fig. 7A, site T5) are compatible with NNE extension. This state of stress is not similar to any tectonic phase previously described, which may be explained by local rotation of the structures.

5.4.4. Wanding fault

The Wanding fault, bounding in the south the Baoshan area, trends EW along the Myanmar/China border in its western part, then curves to the northeast in its eastern part. The fault does not extend beyond the Chong/Lanchang Shan. Along the fault trace, fault scarps and hot springs are common. An historical earthquake occurred close to the Wanding fault and its active left slip displacement is shown by numerous offset streams, up to 10 km (Wang and Burchfiel, 1997). The occurrence of a hairpin loop geometry as the Salween river cross the Wanding fault has been interpreted as the result of two superimposed offsets of opposite sense, the left-lateral movement on the fault over-printing a former right-lateral bend (Lacassin et al., 1998).

Southeast of the curved part of the fault, a fold-and-thrust-belt involving Paleogene rocks is curved and convex to the southeast, whereas structures north of the fault trend N/S and curve only in the western part as described above. This geometry is illustrated on Fig. 7A. The axial traces of curvature on each side of the fault are not in line (west versus southwest). Extensional basins are present along the north-eastern part of the fault (Fig. 7D). The Kejie basin (Fig. 7D), for example, is filled with Paleogene, Neogene and Quaternary sediments. Fault slip analysis in Neogene deposits bounding the basin show a preferential NE direction of left-lateral transtensile faulting and its conjugated right-lateral NW fault direction (Fig. 7A, site T6). This is related with a WNW direction of extension and NNE compression, indicating that the Wanding fault is not a pure strike-slip but rather a transtensile fault. The state of stress responsible for this motion is compatible with that evidenced along the Gaoligong and also with the second motion that affected the Liu Ku fault zone. South of the Wanding fault, various basins were opened and are filled with Paleogene to Quaternary sediments. In the Neogene deposits of the Ke Jie basin, for example, only the last deformation is exposed. This state of stress is close to the one derived from focal mechanisms indicating that it may still be active. On the contrary, the Paleogene basins in this area are offset left-laterally by NW trending faults (Fig. 7D), implying that they have been affected also by the earlier state of stress.

5.5. Nanting fault zone

The Nanting fault extends from the boundary with the Lamping fold and thrust belt in the Yunxian area until Myanmar where it is intersected by the Sagaing fault (Fig. 2). It is marked by characteristic geomorphic features such as stream offset, alluvial fans offset (Wang and Burchfiel, 1997), and is the current locus of important earthquakes which focal mechanism is a left-slip along NE strike (Holt et al., 1991). There are clear indicators of the left-lateral motion along this fault, particularly in its central part. The Menglian ophiolitic suture is offset by 40–50 km, this representing the total offset on the central part of the fault (Wang and Burchfiel, 1997). However, in Myanmar it does not appear to offset the Sagaing fault, thus indicating that connection with this right-lateral fault system is not understood. Landsat TM analysis and field work performed in Myanmar show that the E–W-trending fault has an important normal component, as indicated by large fault scarp (Fig. 10). This variation of motion along the Nanting fault system may be explained by clockwise rotation of blocks along the Nanting fault combined with a drag by the Sagaing fault. This would result in extension in the Bhamo/Mogok area allowing important exhumation, left-lateral strike-slip in the central part of the Nanting fault, and compression and folding in the Yunxian area characterized by the major fold of the Wulian Shan (Fig. 13).

5.6. Gaoligong Shan

The westernmost metamorphic range is the north–south trending Gaoligong Shan (Fig. 8). This range is 3000 meters high and marks the divide between the Long Chuan River in

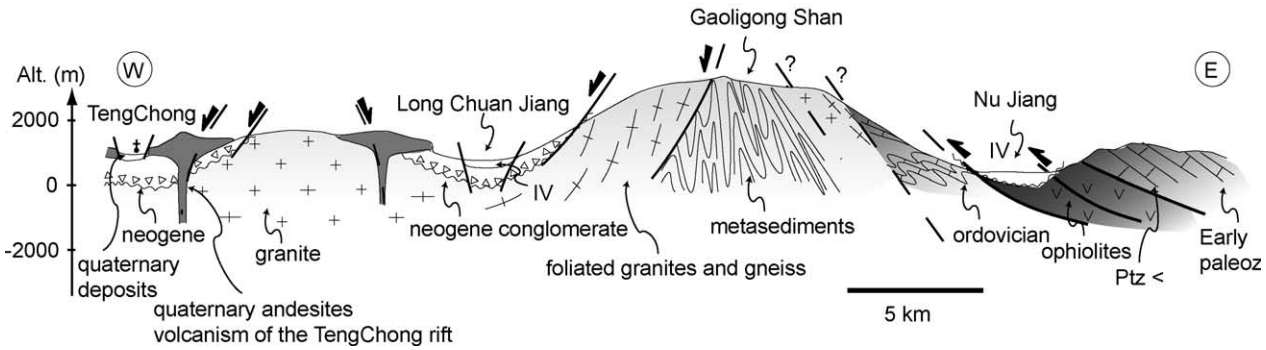

Fig. 8. E–W cross section of the Gaoligong Shan.

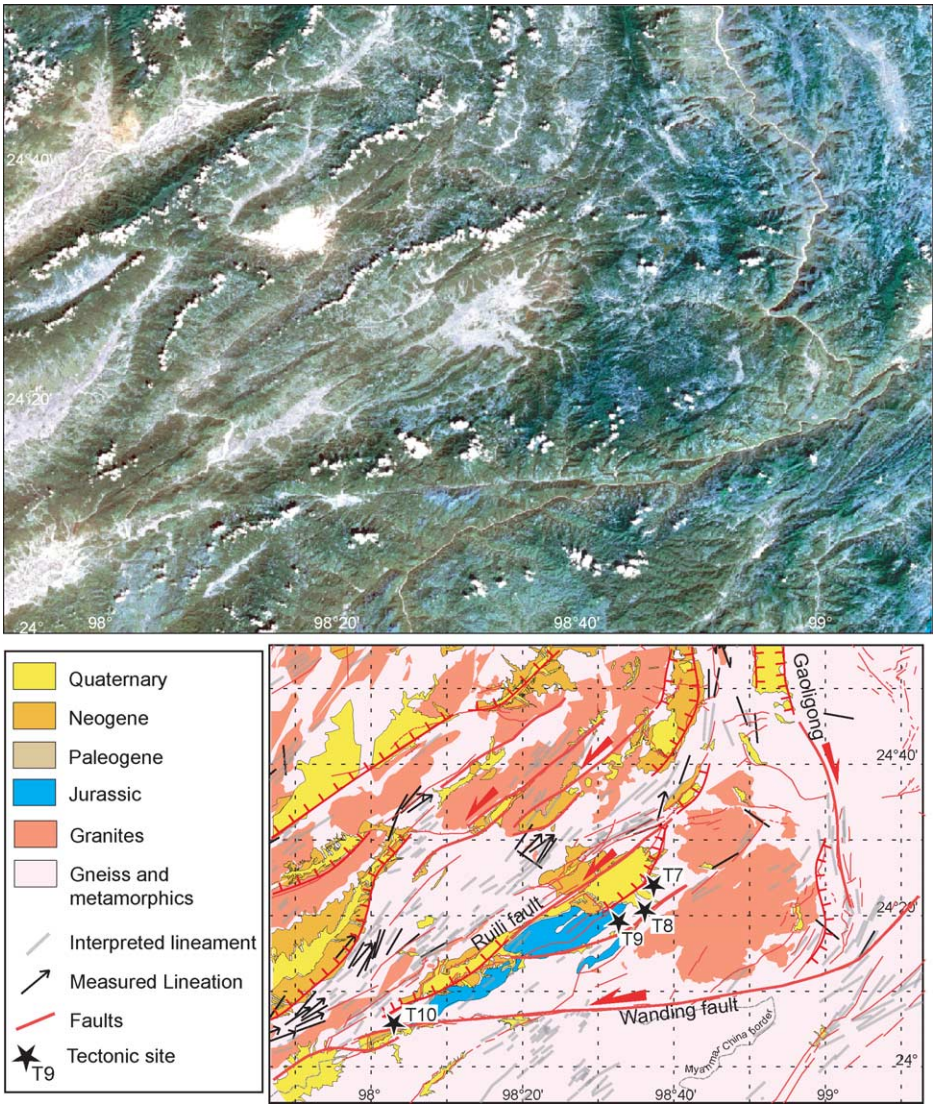

Fig. 9. Tectono-stratigraphic map of the Ruili area from interpretation of Landsat 7 imagery. Left: colour row Landsat 7 satellite image and right: Geologic and tectonic interpretation showing active faults and recent basins opened along the faults, exposed granites and metamorphics with the direction of lineation measured in the field and interpreted from imagery.

the west and the Nu (Salween) River in the east. It limits the Baoshan area and the Tengchong/Ruili area. The core of the range is composed of high-grade metamorphics and foliated granites. They are intensely deformed and affected by a sub-vertical foliation, dipping toward both East and West directions, as well as isoclinal ductile folding. Sheet folds and mineral lineation parallel to the range trend indicate severe stretching. Ductile shear sense criteria show a right-lateral motion. The mylonitization is dated between 12 and 20 Ma (Zhong et al., 1991; Wang and Burchfiel, 1997). East of the range, the metamorphics are probably separated by a detachment fault from the folded Paleozoic sediments of the Baoshan block. Southernmost ophiolitic rocks are pinched between the metamorphic rocks and the Paleozoic sediments. In the western part of the range, foliated granites are exposed. They are overlain by Neogene deposits. Toward the west, the basement, composed of flat foliated granites and metamorphic rocks, is intruded by recent volcanic rocks of the Tengchong rift.

Southward the mylonitic belt disappears near Longling Town. A large batholith intrudes the metamorphic range which seems to curve to the southwest. An earthquake swarm occurred in 1976 ($M = 5.29–7.1$), which have been interpreted to be related to left-lateral movement along NE trending faults (Holt et al., 1991), indicate that this segment of the fault zone is still active.

5.7. Longling-Ruili area

The Longling-Ruili area is mainly composed of foliated granites and gneiss rearranged by NE-trending active faults and overlain by the Neogene and Quaternary basins (Fig. 9).

5.7.1. Ductile deformation of the metamorphic rocks

The basement is constituted by high-grade metamorphic rocks, gneiss and foliated granites. It is the north eastern continuity of the Mogok metamorphic belt of eastern Myanmar but we did not find the metamorphosed sediments exposed in the Mogok area (Fig. 10). Their foliation is rippling around the horizontal. The mineral stretching lineation fluctuates around a N40° direction. Interpreted stretching direction from Landsat 7 imagery (Fig. 9) show that the lineation direction roughly follows the trending direction of the metamorphic range. We performed a set of N/S cross section of this range. Gneisses are in contact with Paleozoic metamorphic sediments, separated by a detachment fault (Fig. 11). The metamorphics and the detachment are unconformably overlain by a N-dipping Neogene conglomerate reworking blocks of metamorphics, in the lowermost deposits of NE-trending basins. Shear criteria, like rolling structures (see photograph on Fig. 11), pressure shadows or S-C shear bands show a constant top to the NE ductile motion. N–S thin sections of the metamorphic rocks all show this sub horizontal foliation, affected by a ductile shear top to the NE.

5.7.2. Ruili fault system

The basement is traversed by several NE-trending faults, mainly dipping to the NW. The faults run parallel to elongate basins on their north western side. The basins present a half grabben shape and contain Pliocene basal lacustrine sediments overlain by the Quaternary deposits. Wang and Burchfiel (1997) showed a left-lateral active motion along these faults. However, the overall geometry of the fault and the structural relationship with the basins suggest a NW–SE extension. Fault-slip data analysis (Fig. 7C) indeed shows a general NW/SE extension with a variable amount of strike-slip, increasing from east to west. In the vicinity of Longling, the Ruili fault is curved toward to the north and seems to connect the Gaoligong boundary faults.

South of Longling, a large granitic intrusive was exhumed along faults related to this NW–SE extension.

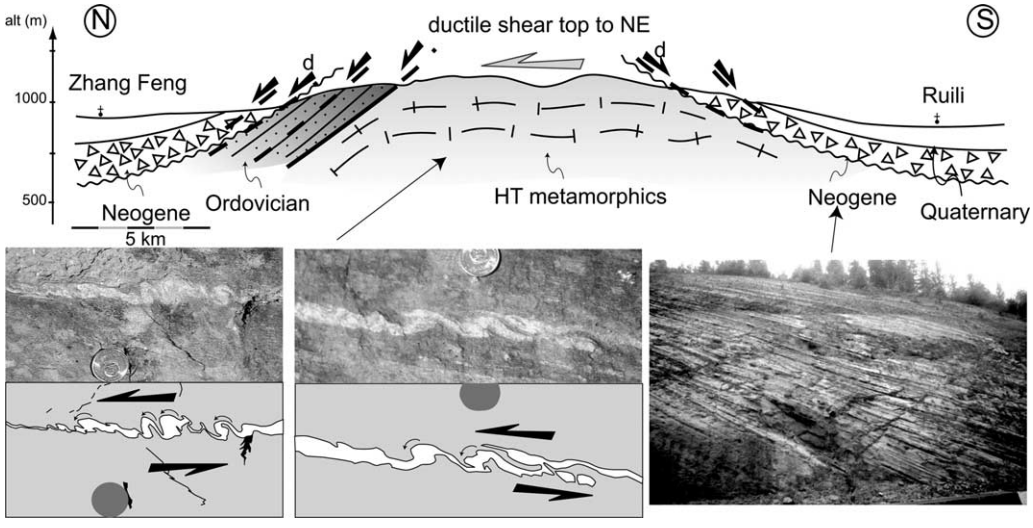

Fig. 10. NNW-SSE schematic cross section of the Mogok high-temperature metamorphic belt (Myanmar).

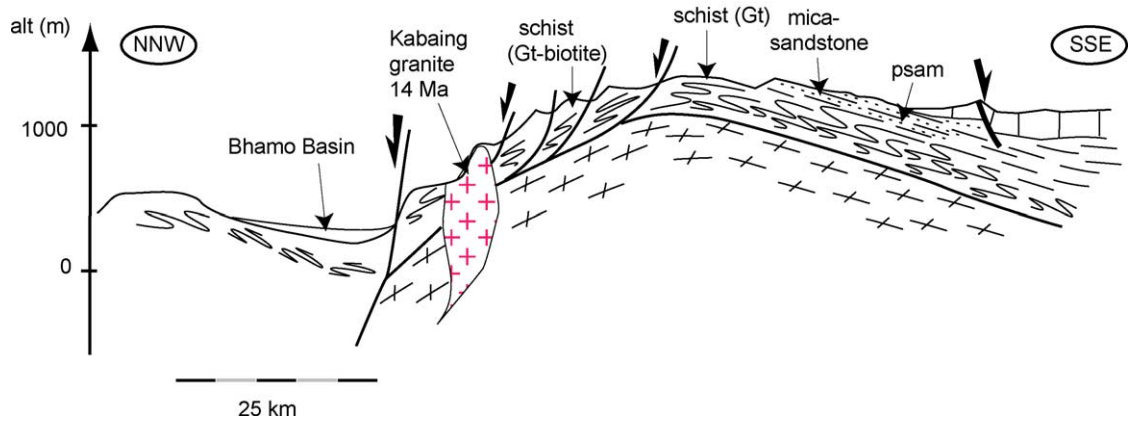

Fig. 11. NE–SW cross section of the metamorphic belt north of Ruili. The photographs and their interpretations show rolling structures in feldspar veins sheared toward the NE and tilted Neogene breccias.

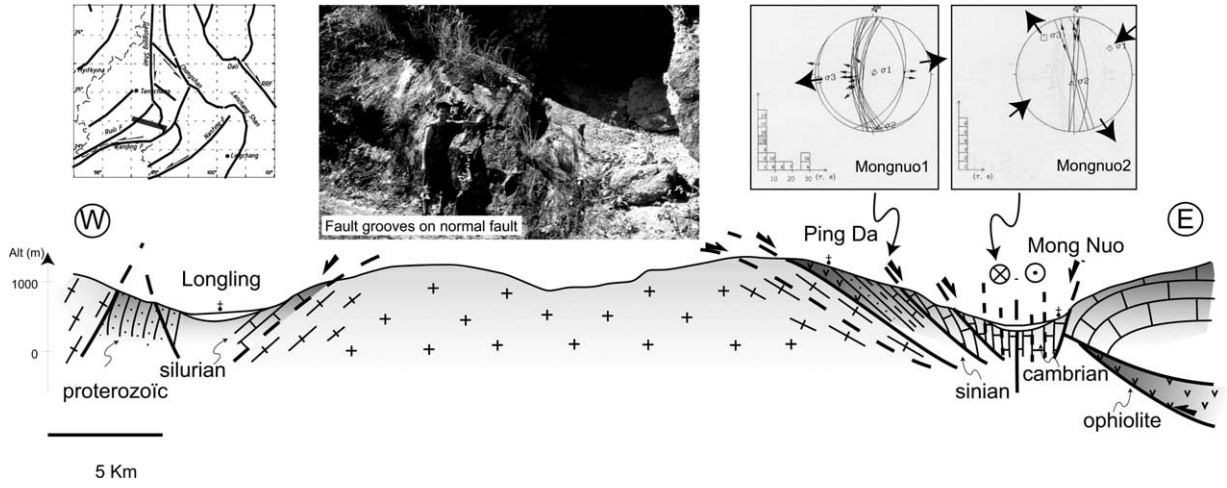

Fig. 12. NW–SE cross section across the granitic pluton south of Longling. The photograph shows a E-dipping grooved normal fault plane. Fault-slip analysis diagrams show the partition of the deformation between N–S trending normal faults and N–S trending right-lateral faults.

On a NW–SE cross section (Fig. 12), the granitic dome exhibits foliation along its eastern border. There, the foliation dips toward to the east and affected by a late normal detachment fault contributing to its exhumation. Fault-slip data analysis (Fig. 12) performed in the valley show that the motion is partitioned between normal component along east-dipping fault and a right-lateral strike-slip along vertical north trending faults parallel to the Gaoligong Shan.

Toward the north, extension is expressed in a large rift basin—the Tengchong rift—where Quaternary volcanic activity occurred. The volcanic rocks are basalts and andesites, dated as Miocene, Pleistocene and Holocene. Isotopic dating reports generally 7.2 Ma (Zhong et al., 1991). The youngest eruption occurred in the 17th century (Wang and Burchfiel, 1997). Volcanic cones are roughly aligned along N/S trend.

6. Conclusion

The large region which occupies the southern part of the Himalayan Syntaxis accommodates the relative displacements between India, Eurasia, Sundaland and South China blocks and underwent ductile and brittle deformation during the Tertiary.

6.1. Ductile deformation

The ductile deformation (Fig. 13) is best illustrated by the ductile left-lateral motion previously described along the Ailao-Diangcan Shan from ~35 to 20 Ma (Leloup et al., 1995). Left-lateral ductile shear is also present in the Chong/Langchan Shan metamorphic belt. The cataclastic deformation in the Chong Shan occurred during the Cenozoic

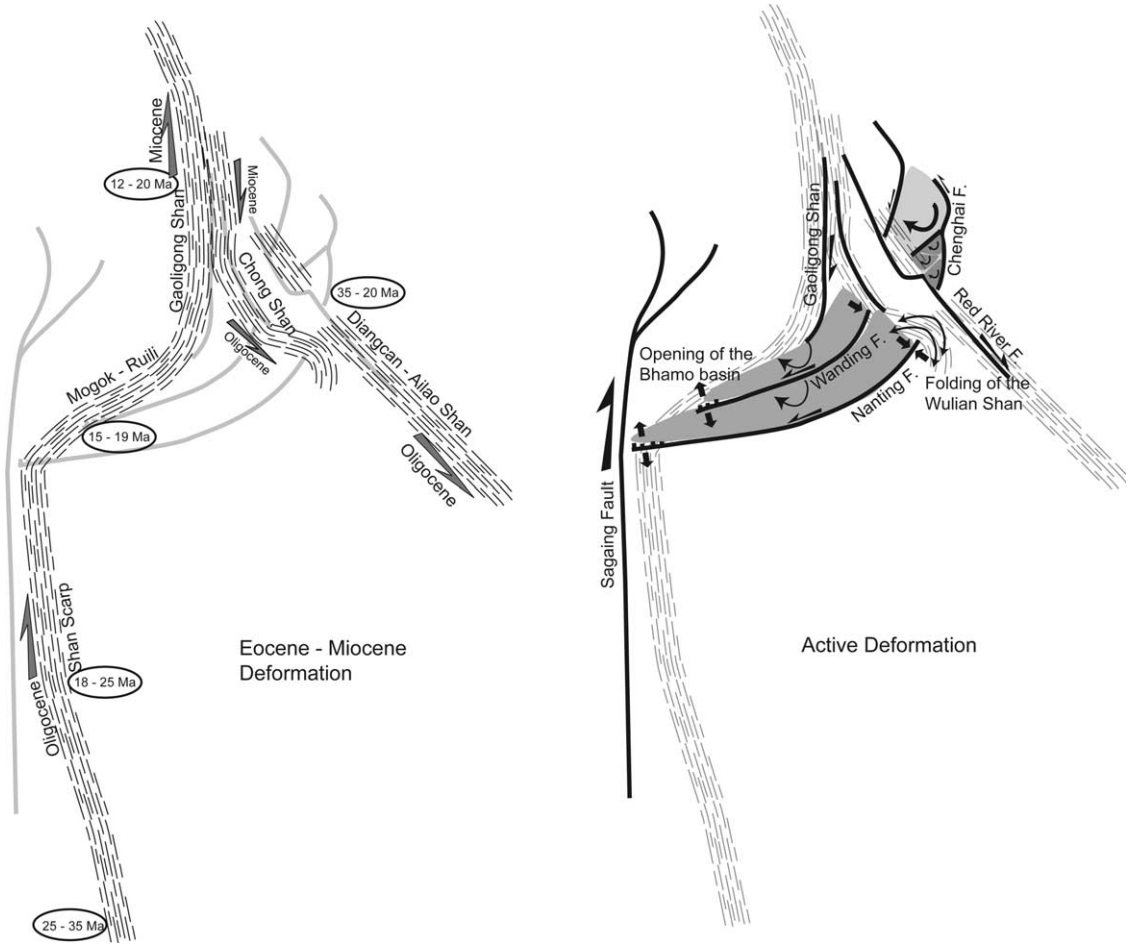

Fig. 13. Active deformation: accommodation of the variation of left lateral slip along Wanding, Nanting and Chenghai faults by clockwise rotation of blocks. This rotation is compatible with a right-lateral drag by the Sagaing fault. The rotation creates extension in the western part with the opening of Bhamo basin and compression in the NE part with folding of the Wulian Shan. Eocene—Miocene deformation: accommodation of relative motion between India, Indochina and South China blocks in ductile shear zones. During Oligocene the Shan Scarp accommodated the right-lateral relative motion between India and Indochina while the Ailao/Diangcan Shan together with Chong Shan accommodated the left-lateral relative motion between Indochina and South China blocks. Later, during the Miocene, this left-lateral strike-slip motion stopped, while the right-lateral shear between India and Indochina migrated northward implying thinning through the Ruili/Mogok area and ductile right lateral shear along the Gaoligong Shan and the Chong Shan.

(Wang and Burchfiel, 1997), and thus may be related to this early stage.

However, we also observe a late dextral ductile-brittle deformation along the Chong Shan. To the West, the Gaoligong Shan was affected by a right-lateral ductile shear dated between 12 and 20 Ma (Zhong et al., 1991; Wang and Burchfiel, 1997). The bending of the Chong Shan range and late right-lateral shear could be explained by a drag of the Chong Shan by the motion of the Gaoligong Shan.

The Gaoligong Shan is connected to its Myanmar equivalent, the Shan Scarp, by the Mogok/Ruili metamorphic belt, where high-grade metasediments, gneisses and foliated granites are exposed. We observe that in the Ruili area the ductile deformation occurred on a flat schistosity with top to the NE motion. This belt connects in Myanmar the ruby-bearing Mogok metamorphic belt and the Shan Scarp further to the south. In the Mogok area we evidenced N to NE foliation associated to a top-to-the-N motion and normal faults. This is in favour of crustal thinning and extension and exhumation of the metamorphic rocks. Along the Shan Scarp the right-lateral motion is accommodated in wrench and was dated from 30 Ma in southern Myanmar to 15 Ma in the Mogok area, which has been interpreted as the northward migration of a crustal thinning (Bertrand et al., 2001) in response to the northward migration of India. The Gaoligong belt, together with its Myanmar equivalents, the Shan Scarp and Mogok/Ruili metamorphic belts, constituted the major strike-slip boundary between Indochina and India, in ductile deformation, involving both tangential and wrench motion expressed at mid-crustal level and later exhumed. The Mogok/Ruili belt may be interpreted as an extensional releasing bend between the Shan Scarp and the Gaoligong belt.

6.2. Brittle deformation

We individualized two brittle deformation events. The first one is an ENE to E–W compression associated with NNW extension, compatible with left-lateral wrench along NW-trending faults which offset the Chong Shan and affect Paleogene sediments. This state of stress could thus be coeval with the left-lateral ductile motion evidenced on the Chong Shan and the Ailao/Diangcan Shan.

The second event is a well-marked WNW to E–W extension, affecting Neogene deposits, which accounts for right-lateral strike-slip on the Gaoligong and left-lateral transtensile NE–SW faults such as the Nanting, Wanding and Ruili faults. This state of stress is close to the one derived from focal mechanisms and might then be still active.

6.3. Interpretation

During Eocene to Miocene time, NE corner of the Indian plate was situated over 1000 km south of its present position. The northern termination of Sunda Plate (Three Rivers area) was wedged during the Tertiary between the left-lateral Ailao Shan/Chong Shan metamorphic belts to the east and the right-lateral Shan scarp/Gaoligong metamorphic belt in west. This triangular region therefore underwent the effects of these continental size ductile strike-slip faults separating major blocks with a dominant EW to ENE compression. The Shan Scarp constituted the major strike-slip boundary between Indochina and India, and accommodated in right-lateral wrench. At the same time the Ailao/Diangcan Shan and the Chong Shan zones were sheared left-laterally allowing the displacement toward the SE of Indochina block relative to South China. The area covered by the Yunnan Province was situated NE of the Eastern Himalayan Syntaxis, and occupied a geographic position which is that of the Present-day Sichuan Province. An analogy can be made between the assemblage of structures in southwestern Sichuan and the Eocene to Miocene structures of western Yunnan (Wang and Burchfiel, 2000). If we compare the first state of stress that we obtained from fault slip analysis and the state of stress derived from focal mechanisms in Sichuan, we see that stress directions (ENE compression associated to a NNW extension) are coaxial. This suggests that crust initially situated NE of the syntaxis undergo this E–W compression, prior to the rotation of the stress principal axes, and finally NW–SE relaxation, past the Syntaxis.

In the Miocene, ductile deformation terminated on Ailao/Diangcan Shan. However, it migrated north along the Shan Scarp to the Mogok/Ruili metamorphic belt and the Gaoligong belt (Fig. 13), dragging the Chong Shan right-laterally and overprinting a late right-lateral ductile deformation on its metamorphic rocks and opening northern Myanmar basins.

The late Neogene to present system might have been active since the late Miocene/Pliocene. We regard it as a combination of the right-lateral Sagaing Fault/Gaoligong, which propagates toward the north as a horse tail, and the circum syntaxis fault system. The state of stress is a N–S compression which a regional characteristic of the northern part of the Sunda block and a WNW extension inferred from both focal mechanisms and recent fault-slip data analysis. We propose that this interaction is accommodated by clockwise rotations of blocks (Fig. 13). In the Dali area, for example, small blocks abut the Ailao Shan/Red River Fault sliding along the left-lateral circum syntaxis faults termination (Chenghai fault). This geometry accounts for the deformation pattern between the Chong Shan and the Sagaing fault where blocks are dragged by the right lateral shear of this system. It also created extension in the Bhamo/Mogok area allowing important exhumation, left-lateral strike-slip in the central part of the Nanting and Wanding faults and compression and folding in the Wuglian Shan.

Acknowledgements

Field work in Yunnan was supported by Ecole Normale Supérieure. We are grateful to the Chengdu Institute of Technology for logistic assistance. This paper also makes use of observations in the field in Myanmar within the framework of the EEC/ASEAN GEODYSSEA program and the GIAC Program coordinated by C. Rangin in conjunction with TMEP, MOGI, and the Universities of Yangon and Mandalay. We benefited from useful reviews from Dr Shrivastava and Dr Kumar. M.P. belongs to the Centre National de la Recherche Scientifique (CNRS/UMR8538).

References

Achache, J., Courtillot, V., Zhou, Y.X., 1984. Paleogeographic and tectonic evolution of southern Tibet since middle Cretaceous time—new paleomagnetic data and synthesis. Journal of Geophysical Research 89 (B12), 311–339.

BGMRY, 1983. Geological map of Yunnan. Bureau of Geology and Mineral Resources of Yunnan, 1:500000 1983.

BGMRY, 1990. Regional Geology of Yunnan Province (Brief text in English), in: Bureau of Geology and Mineral Resources of Yunnan Provice (Ed.), Regional geology of Yunnan Province Geological memoirs. Geological Publishing House, Beijing, pp. 658–728.

Bertrand, G., Rangin, C., Maluski, H., Han, T.A., Thein, M., Myint, O., Maw, W., Lwin, S., 1999. Cenozoic metamorphism along the Shan scarp (Myanmar): evidences for ductile shear along the Sagaing fault or the northward migration of the eastern Himalayan syntaxis. Geophysical Research Letters 26 (7), 915–918.

Bertrand, G., Rangin, C., Maluski, H., Bellon, H., 2001. Diachronous cooling along the Mogok metamorphic belt (Shan scarp, Myanmar): the trace of the northward migration of the Indian syntaxis. Journal of Asian Earth Sciences 19 (5), 649–659.

Bilham, R., Larson, K., Freymueller, J., Jouanne, F., LeFort, P., Leturmy, P., Mugnier, J.L., Gamond, J.F., Glot, J.P., Martinod, J., Chaudury, N.L., Chitrakar, G.R., Gautam, U.P., Koirala, B.P., Pandey, M.R., Ranabhat, R., Sapkota, S.N., Shrestha, P.L., Thakuri, M.C., Timilsina, U.R., Tiwari, D.R., Vidal, G., Vigny, C., Galy, A., deVoogd, B., 1997. GPS measurements of present-day convergence across the Nepal Himalaya. Nature 386 (6620), 61–64.

Careygailhardis, E., Mercier, J.L., 1987. A numerical-method for determining the state of stress using focal mechanisms of earthquake populations—application to Tibetan Teleseisms and Microseismicity of southern Peru. Earth and Planetary Science Letters 82 (1–2), 165–179.

Chen, Z., Burchfiel, B.C., Liu, Y., King, R.W., Royden, L.H., Tang, W., Wang, E., Zhao, J., Zhang, X., 2000. Global positioning system measurements from eastern Tibet and their implications for India/Eurasia intercontinental deformation. Journal of Geophysical Research-Solid Earth 105 (B7), 16215–16227.

Davy, P., Cobbold, P.R., 1991. Experiments on shortening of a 4-layer model of the continental lithosphere. Tectonophysics 188 (1–2), 1–25.

DeMets, C., Gordon, R.G., Argus, D.F., Stein, S., 1994. Effect of recent revisions to the geomagnetic reversal time scale on estimates of current plate motions. Geophysical Research Letters 21 (20), 2191–2194.

Dewey, J.F., Cande, S.5C., Pitman III., W.C., 1989. Tectonic evolution of the India/Eurasia collision zone. Eclogae Geologicae Helvetiae 82 (3), 717–734.

England, P., Houseman, G., 1986. Finite strain calculations of continental deformation. 2. Comparison with the India-Asia collision zone. Journal of Geophysical Research-Solid Earth and Planets 91 (B3), 3664–3676.

England, P., McKenzie, D., 1982. A thin viscous sheet model for continental deformation. Geophysical Journal of the Royal Astronomical Society 70 (2), 295–321.

Garzanti, E., Critelli, S., Ingersoll, R.V., 1996. Paleogeographic and paleotectonic evolution of the Himalayan range as reflected by detrital modes of Tertiary sandstones and modern sands (Indus transect, India and Pakistan). Geological Society of America Bulletin 108 (6), 631–642.

Hallet, B., Molnar, P., 2001. Distorted drainage basins as markers of crustal strain east of the Himalaya. Journal of Geophysical Research, B, Solid Earth and Planets 106 (7), 13697–13709.

Holt, W.E., Ni, J.F., Wallace, T.C., Haines, A.J., 1991. The active tectonics of the eastern Himalayan syntaxis and surrounding regions. Journal of Geophysical Research, B, Solid Earth and Planets 96 (9), 14595–14632.

Holt, W.E., Li, M., Haines, A.J., Anonymous, 1995. Mapping the complete horizontal velocity gradient field in Asi=a=20 using constraints from earthquake moment tensors, Quaternary=20 deformation rates, VLBI measurements, and rigid plate kinematics. International Union of Geodesy and Geophysics; XXI General Assembly 21, 360. Week B.

Houseman, G., England, P., 1986a. A dynamic-model of lithosphere extension and sedimentary basin formation. Journal of Geophysical Research-Solid Earth and Planets 91 (B1), 719–729.

Houseman, G., England, P., 1986b. Finite strain calculations of continental deformation. 1. Method and general results for convergent zones. Journal of Geophysical Research-Solid Earth and Planets 91 (B3), 3651–3663.

Houseman, G., England, P., 1993. Crustal thickening versus lateral expulsion in the Indian–Asian continental collision. Journal of Geophysical Research-Solid Earth 98 (B7), 12233–12249.

Houseman, G.A., Molnar, P., Miller, J.A.e., Holdsworth, R.E.e., Buick, I.S.e., Hand, M.e., 2001. Mechanisms of lithospheric rejuvenation associated with continental orogeny. Continental reactivation and reworking. Orogenesis in the Outback 184, 13–38.

Huchon, P., Lepichon, X., Rangin, C., 1994. Indo-China Peninsula and the collision of India and Eurasia. Geology 22 (1), 27–30.

Jolivet, L., 2001. A comparison of geodetic and finite strain pattern in the Aegean, geodynamic implications. Earth and Planetary Science Letters 187 (1–2), 95–104.

Jolivet, L., Davy, P., Cobbold, P., 1990. Right-lateral shear along the northwest pacific margin and the India-Eurasia collision. Tectonics 9 (6), 1409–1419.

Lacassin, R., Replumaz, A., Leloup, P.H., 1998. Hairpin river loops and slip-sense inversion on southeast Asian strike-slip faults. Geology 26 (8), 703–706.

Leloup, P.H., Harrison, T.M., Ryerson, F.J., Chen, W.J., Li, Q., Tapponnier, P., Lacassin, R., 1993. Structural petrological and thermal evolution of a Tertiary ductile strike-slip shear zone, Diancang Shan, Yunnan. Journal of Geophysical Research-Solid Earth 98 (B4), 6715–6743.

Leloup, P.H., Lacassin, R., Tapponnier, P., Scharer, U., Zhong, D.L., Liu, X.H., Zhang, L.S., Ji, S.C., Trinh, P.T., 1995. The Ailao Shan-Red River shear zone (Yunnan, China), Tertiary transform boundary of Indochina. Tectonophysics 251 (1–4), 3–84.

Metcalfe, I., 1996. Gondwanaland dispersion, Asian accretion and evolution of eastern Tethys. Australian Journal of Earth Sciences 43 (6), 605–623.

Metcalfe, I., Spiller, F.C.P., Benpei, L., Haoruo, W., Sashida, K., 1999. The Palaeo-Tethys in Mainland East and Southeast Asia: contributions from radiolarian studies, in: Metcalfe, I. (Ed.), Gondwana dispersion and Asian accretion, Final Results Volume for IGCP Project 321. A.A. Balkema, Rotterdam, pp. 259–281.

Michel, G.W., Yu, Y.Q., Zhu, S.Y., Reigber, C., Becker, M., Reinhart, E., Simons, W., Ambrosius, B., Vigny, C., Chamot-Rooke, N., Le Pichon, X., Morgan, P., Matheussen, S., 2001. Crustal motion and block behaviour in SE-Asia from GPS measurements. Earth and Planetary Science Letters 187 (3–4), 239–244.

Molnar, P., Lyon-Caen, H., 1989. Fault plane solutions of earthquakes and active tectonics of the Tibetan Plteau and its margins. Geophysical Journal of the Royal Astronomical Society 99 (1), 123–153.

Molnar, P., Tapponnier, P., 1975. Cenozoic tectonics of Asia; effects of a continental collision. Science 189 (4201), 419–426.

Molnar, P., Tapponnier, P., 1977. Relation of the tectonics of eastern China to the India-Eurasia collision; application of slip-line field theory to large-scale continental tectonics. Geology (Boulder) 5 (4), 212–216.

Morley, C.K., 2001. Combined escape tectonics and subduction rollback-back arc extension; a model for the evolution of Tertiary rift basins in Thailand Malaysia and Laos. Journal of the Geological Society of London 158 (Part 3), 461–474.

Morley, C.K., 2002. A tectonic model for the Tertiary evolution of strike-slip faults and rift basins in SE Asia. Tectonophysics 347 (4), 189–215.

Morley, C.K., Woganan, N., Sankumarn, N., Hoon, T.B., Alief, A., Simmons, M., 2001. Late Oligocene–Recent stress evolution in rift basins of northern and central Thailand; implications for escape tectonics. Tectonophysics 334 (2), 115–150.

Paul, J., Buergmann, R., Gaur, V.K., Bilham, R., Larson, K.M., Ananda, M.B., Jade, S., Mukal, M., Anupama, T.S., Satyal, G., Kumar, D., 2001. The motion and active deformation of India. Geophysical Research Letters 28 (4), 647–650.

Pubellier, M., Ego, F., 2002. Anatomy of an escape tectonic zone: Western Irian Jaya (Indonesia). Tectonics 21 (4) art. no.-1019.

Rangin, C., Maw, W., Lwin, S., Naing, W., Mouret, C., Bertrand, G., Anonymous, 1999. Cenozoic pull-apart basins in central Myanmar; the trace of the path of India along the western margin of Sundaland, in: European Union of Geosciences Conference; EUG 10. Strasbourg, France, p. 59.

Ratschbacher, L., Frisch, W., Linzer, H.-G., Merle, O., 1991. Lateral extrusion in the eastern Alps; Part 2, Structural analysis. Tectonics 10 (2), 257–271.

Ratschbacher, L., Frisch, W., Chen, C., Pan, G., 1996. Cenozoic deformation, rotation and stress patterns in eastern Tibet and western Sichuan, China, in: AYH (Ed.), The Tectonic Evolution of Asia, pp. 227–249.

Replumaz, A., Lacassin, R., Tapponnier, P., Leloup, P.H., 2001. Large river offsets and Plio-Quaternary dextral slip rate on the Red River fault (Yunnan, China). Journal of Geophysical Research-Solid Earth 106 (B1), 819–836.

Sato, K., Yuyan, L., Zhicheng, Z., Yang, Z., Otofuji, Y.-i., 2001. Tertiary paleomagnetic data from northwestern Yunnan, China; further evidence for large clockwise rotation of the Indochina block and its tectonic implications. Earth and Planetary Science Letters 185 (1–2), 185–198.

Searle, M.P., 1991. Precollision and postcollision thermal events in the Himalaya: comment. Geology (Boulder) 19 (6), 666–667.

Simons, W.J.F., Ambrosius, B.A.C., Noomen, R., Angermann, D., Wilson, P., Becker, M., Reinhart, E., Walpersdorf, A., Vigny, C., 1999. Observing plate motions in Southeast Asia; geodetic results of the GEODYSSEA Project. Geophysical Research Letters 26 (14), 2081–2084.

Socquet, A., Goffe, B., Pubellier, M., Rangin, C., 2002a. Late Cretaceous to Eocene metamorphism of the internal zone of the Indo-Burma range (western Myanmar): geodynamic implications. Comptes Rendus Geoscience 334 (8), 573–580.

Socquet, A., Vigny, C., Pubellier, M., Rangin, C., 2002b. Accommodation of the relative motion between India and Sundaland, in: AGU (Ed.), Western Pacific Geophysics Meeting. Wellington, New Zealand.

Socquet, A., Vigny, C., Simons, W., Chamot-Rooke, N., Rangin, C., Ambrosius, B., 2004. GPS determination of the relative motion between India and Sunda and its accommodation in Myanmar. Journal of Geophysical Research, submitted for pulication.

Tapponnier, P., Molnar, P., 1977. Rigid plastic indentation; the origin of syntaxis in the Himalayan Belt Himalaya; sciences de la terre, in: Jest, C. (Ed.), Ecologie et geologie de l'Himalaya, pp. 431–432. Paris, France.

Tapponnier, R., Peltzer, G., Le Dain, A.Y., Armijo, R., Cobbold, P., 1982. Propagating extrusion tectonics in Asia; new insights from simple experiments with plasticine. Geology (Boulder) 10 (12), 611–616.

Tapponnier, P., Xu, Z.Q., Roger, F., Meyer, B., Arnaud, N., Wittlinger, G., Yang, J.S., 2001. Geology—oblique stepwise rise and growth of the Tibet plateau. Science 294 (5547), 1671–1677.

Wang, E., Burchfiel, B.C., 1997. Interpretation of Cenozoic tectonics in the right-lateral accommodation zone between the Ailao Shan shear zone and the eastern Himalayan syntaxis. International Geology Review 39 (3), 191–219.

Wang, E., Burchfiel, B.C., 2000. Late Cenozoic to Holocene deformation in southwestern Sichuan and adjacent Yunnan China, and its role in formation of the southeastern part of the Tibetan Plateau. Geological Society of America Bulletin 112 (3), 413–423.

Wang, E., Burchfiel, B.C., Royden, L.H., Liangzhong, C., Jishen, C., Wenxin, L., Zhiliang, C., 1998. Late Cenozoic Xianshuihe-Xiaojiang Red River, and Dali fault systems of southwestern Sichuan and central Yunnan, China. Special Paper—Geological Society of America 327, 108.

Wang, Q., Zhang, P.Z., Freymueller, J.T., Bilham, R., Larson, K.M., Lai, X., You, X.Z., Niu, Z.J., Wu, J.C., Li, Y.X., Liu, J.N., Yang, Z.Q., Chen, Q.Z., 2001. Present-day crustal deformation in China constrained by global positioning system measurements. Science 294 (5542), 574–577.

Zhong, D., Wang, Y., Ding, L., 1991. The Tertiary Gaoligong intra-continental strike-slip fault and its associated extensional structure in western Yunnan, China, in: Zhang X. (Ed.), Annual report 1989–1990 Lab. Lithos. Tecton. Evolution. Inst. Geol., Academia Sinica, Beijing, pp. 18–22.